

# Strain correlations in isotropic elastic bodies

J.P. Wittmer,<sup>1,\*</sup> A.N. Semenov,<sup>1</sup> and J. Baschnagel<sup>1</sup>

<sup>1</sup>*Institut Charles Sadron, Université de Strasbourg & CNRS,  
23 rue du Loess, 67034 Strasbourg Cedex, France*

(Dated: March 31, 2023)

Strain correlation functions in two-dimensional isotropic elastic bodies are shown both theoretically (using the general structure of isotropic tensor fields) and numerically (using a glass-forming model system) to depend on the coordinates of the field variable (position vector  $\mathbf{r}$  in real space or wavevector  $\mathbf{q}$  in reciprocal space) and thus on the direction of the field vector and the orientation of the coordinate system. Since the fluctuations of the longitudinal and transverse components of the strain field in reciprocal space are known in the long-wavelength limit from the equipartition theorem, all correlation functions are imposed and no additional physical assumptions are needed.

*Background.* A tensor field assigns a tensor to each point of the mathematical space, in our case for simplicity a two-dimensional Euclidean vector space with Cartesian coordinates and an orthonormal tensor basis [1–3]. Tensor fields are used in differential geometry [1], general relativity [4, 5], in the analysis of stress and strain in materials [6–8] and in numerous other applications in science and engineering. Tensor fields are experimentally [9, 10] or numerically [11–31] probed by means of correlation functions [32–34] of their components and, importantly, these correlation functions are themselves components of tensor fields. See Appendix A for details. Assuming translational invariance, correlation functions are naturally best analyzed (both for theoretical and numerical reasons) in a first step in reciprocal space as functions of the wavevector  $\mathbf{q}$  from which the dependence on the spatial field vector  $\mathbf{r}$  in real space can then be deduced by inverse Fourier transformation [16, 17, 19].

*Investigated case study.* For instance, the correlation functions  $c_{\alpha\beta\gamma\delta}(\mathbf{r}) = \mathcal{F}^{-1}[c_{\alpha\beta\gamma\delta}(\mathbf{q})]$  of the instantaneous strain tensor field  $\varepsilon_{\alpha\beta}(\mathbf{r})$  in real space may be obtained from  $c_{\alpha\beta\gamma\delta}(\mathbf{q}) = \langle \varepsilon_{\alpha\beta}(\mathbf{q}) \varepsilon_{\gamma\delta}(-\mathbf{q}) \rangle$  in reciprocal space with  $\varepsilon_{\alpha\beta}(\mathbf{q}) = \mathcal{F}[\varepsilon_{\alpha\beta}(\mathbf{r})]$  being the Fourier transformed strain tensor field components (cf. Appendix B). (The average  $\langle \dots \rangle$  will be specified below.) An example for the autocorrelation function  $c_{1212}(\mathbf{r})$  of the shear strain  $\varepsilon_{12}(\mathbf{r})$  is given in Fig. 1 obtained numerically for a two-dimensional (effectively) elastic body formed by polydisperse Lennard-Jones (pLJ) particles deep in the glass regime. Interestingly, the correlation function is seen to strongly depend both on the orientation of the field vector  $\mathbf{r}$  (panel (a)) and on the rotation angle  $\alpha$  of the coordinate system (panel (b)). Since the simulated system can be shown to be perfectly isotropic down to a few particle diameters [17, 19, 35–38], these findings beg for an explanation. Expanding on our recent work on spatial correlations of (time-averaged) stress tensor components [16, 17, 19] this behavior is traced back to the fact that correlation functions of tensor fields of isotropic

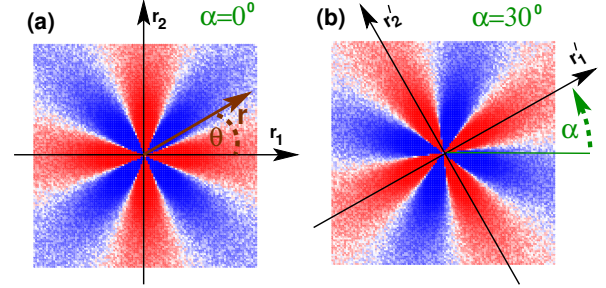


FIG. 1: Autocorrelation function  $c_{1212}(\mathbf{r})$  of the strain field component  $\varepsilon_{12}(\mathbf{r})$  of a generic isotropic elastic body in two dimensions: (a) Unrotated frame with coordinates  $(r_1, r_2)$ , (b) frame  $(r'_1, r'_2)$  rotated by an angle  $\alpha = 30^\circ$  (rotations marked by “r”). Albeit the system is isotropic, the correlation function is strongly angle dependent, revealing an octupolar symmetry. While each pixel corresponds in (a) and (b) to the same spatial position  $\mathbf{r}$ , the correlation functions differ by the angle  $\alpha$ .  $c_{1212}(\mathbf{r})$  is positive (red) along the axes and negative (blue) along the bisection lines of the respective axes.

systems must be components of a generic *isotropic* tensor field. This field is shown to be completely described in terms of only two scalar “invariant correlation functions” (ICFs)  $c_L(q)$  and  $c_T(q)$  in reciprocal space ( $q = |\mathbf{q}|$  being the magnitude of the wavevector), characterizing the independent fluctuations of the longitudinal and transverse strain components  $\varepsilon_L(\mathbf{q})$  and  $\varepsilon_T(\mathbf{q})$  with respect to  $\mathbf{q}$ . Since due to the equipartition theorem of statistical physics  $c_L(q)$  and  $c_T(q)$  are given in the large-wavelength limit ( $q \rightarrow 0$ ) by the macroscopic Lamé coefficients  $\lambda$  and  $\mu$  [6, 9, 10, 21], all strain correlation functions are known on large scales. In turn this explains the octupolar pattern observed in Fig. 1 and shows that strain correlations in elastic bodies must necessarily be long-ranged.

*Outline.* We begin by summarizing some pertinent properties of isotropic tensor fields. Technical points concerning the model system and the data production of tensorial fields in various coordinate systems are discussed thereafter. This is followed by the presentation of our main numerical results, a summary and an outlook. More details may be found in the Appendix both on the theoretical background (cf. Appendices A, E, F and G)

\*Electronic address: joachim.wittmer@ics-cnrs.unistra.fr

and on computational issues (cf. Appendices B, C and D). The strain response due to an imposed stress point source is discussed in Appendix G.

*Isotropic tensor fields.* Isotropic systems, such as generic isotropic elastic bodies [6–8], simple and complex fluids [33, 39, 40], amorphous metals and glasses [23–31, 41], foams and emulsions [20, 22] or, as a matter of fact, our entire universe [4] are described at least on some scales by *isotropic tensors* and *isotropic tensor fields* (cf. Appendix A 2) [1, 3, 8]. It is well known [3, 8] that the components of isotropic tensors remain unchanged under an orthogonal coordinate transformation (including rotations and reflections). For instance,  $E_{\alpha\beta\gamma\delta}^* = E_{\alpha\beta\gamma\delta}$  for the forth-order elastic modulus tensor of an isotropic body (cf. Appendix D) [7, 8] with “\*” marking an arbitrary orthogonal transformation. This implies (cf. Appendix A 4) that  $E_{\alpha\beta\gamma\delta}$  is given by two invariants, e.g., the two Lamé coefficients  $\lambda$  and  $\mu$  being invariant material properties. Importantly, this does *not* hold for isotropic tensor fields [3, 16, 19]. For instance, for a forth-order correlation function in reciprocal space the isotropy condition becomes

$$c_{\alpha\beta\gamma\delta}^*(\mathbf{q}) = c_{\alpha\beta\gamma\delta}(\mathbf{q}^*) \quad (1)$$

with  $\mathbf{q}^*$  being the “actively” transformed wavevector (cf. Appendix A 2). Assuming in addition the system to be achiral and two-dimensional it can be shown (cf. Appendix A 5) that correlation functions of second-order tensor field components must take the following generic structure

$$\begin{aligned} c_{\alpha\beta\gamma\delta}(\mathbf{q}) = & [c_2(q) - 2c_T(q)] \delta_{\alpha\beta}\delta_{\gamma\delta} \\ & + c_T(q) [\delta_{\alpha\gamma}\delta_{\beta\delta} + \delta_{\alpha\delta}\delta_{\beta\gamma}] \\ & + [c_{\perp}(q) - c_2(q) + 2c_T(q)] [\hat{q}_{\alpha}\hat{q}_{\beta}\delta_{\gamma\delta} + \hat{q}_{\gamma}\hat{q}_{\delta}\delta_{\alpha\beta}] \\ & + [c_L(q) + c_2(q) - 2c_{\perp}(q) - 4c_T(q)] \hat{q}_{\alpha}\hat{q}_{\beta}\hat{q}_{\gamma}\hat{q}_{\delta} \end{aligned} \quad (2)$$

in terms of the four ICFs  $c_L(q)$ ,  $c_T(q)$ ,  $c_2(q)$  and  $c_{\perp}(q)$ . Legitimate correlation functions of isotropic systems may thus depend on the coordinates  $\hat{q}_{\alpha}$  of the normalized wavevector  $\hat{\mathbf{q}}$  and, hence, on the orientation of the wavevector and of the coordinate system. While the isotropy of the system may not be manifested by *one* correlation function, it is crucial for the structure of the *complete set* of *all* correlation functions, Eq. (2).

*Technical issues.* We investigate amorphous glasses in two dimensions formed by pLJ particles [17, 19, 35–38, 42] sampled by means of Monte Carlo (MC) simulations [32]. See Appendix C for details (Hamiltonian, units, cooling and equilibration procedure, data production, generation and analysis of tensor fields on discrete grids). Lennard-Jones units are used [32] and all times are given in local MC steps (MCS). We focus on systems containing  $n = 10000$  and  $40000$  particles at a working temperature  $T = 0.2$ . This is much lower than the glass transition temperature  $T_g \approx 0.26$  [35], i.e. for any computationally feasible production time the systems behave as solid elastic bodies [37].  $N_c = 200$  completely independent configurations  $c$  are prepared using a mix of local

and swap MC hopping moves [37, 43] while the presented data are computed only using local MC moves. For each  $c$  we store time-series containing each  $N_t = 10000$  frames  $t$ . As described in Appendix D, the elastic modulus tensor  $E_{\alpha\beta\gamma\delta}$  is isotropic and determined by the two Lamé coefficients  $\lambda \approx 38$  and  $\mu \approx 14$  [35, 37]. To store and to manipulate the various fields needed for the microscopic description a discrete grid of lattice constant  $a_{\text{grid}} \approx 0.2$  is used for all systems (cf. Appendix C 3). The displacement field  $\mathbf{u}(\mathbf{r})$  in real space is determined for each frame  $t$  using a standard method (cf. Appendix E 1) [9, 10, 21] from the particle displacement vectors where we use as reference the time-averaged position of the particles. We obtain then from the Fourier transformed displacement field  $\mathbf{u}(\mathbf{q}) = \mathcal{F}[\mathbf{u}(\mathbf{r})]$  the (linearized) strain tensor field  $\varepsilon_{\alpha\beta}(\mathbf{q})$  [7, 16]. Using the correlation function theorem for Fourier transforms (cf. Appendix B 1) the strain correlations functions in reciprocal space are given by  $c_{\alpha\beta\gamma\delta}(\mathbf{q}) = \langle \varepsilon_{\alpha\beta}(\mathbf{q}) \varepsilon_{\gamma\delta}(-\mathbf{q}) \rangle$  where the average is taken over all  $t$  and  $c$ . Both strain and correlation function fields in reciprocal space are defined to be dimensionless (cf. Appendix B 1). We emphasize by a prime “ $r$ ” all tensor field components obtained in a coordinate system rotated by an angle  $\alpha$ . ( $\alpha = 0$  being the original unrotated system). Specifically, the correlation functions  $c'_{\alpha\beta\gamma\delta}(\mathbf{q}) = \langle \varepsilon'_{\alpha\beta}(\mathbf{q}) \varepsilon'_{\gamma\delta}(-\mathbf{q}) \rangle$  are obtained using the components  $u'_{\alpha}(\mathbf{r})$  and  $q'_{\alpha}$  in the rotated frame.

*Natural Rotated Coordinates (NRC).* All the tensorial fields introduced above depend on the orientation of the coordinate system. Importantly, we consider these properties in a first step in “Natural Rotated Coordinates” (NRC) where for *each* wavevector  $\mathbf{q}$  the coordinate system is rotated until the 1-axis coincides with the  $\mathbf{q}$ -direction. We mark these new tensor field components by “o” to distinguish them from standard rotated tensor field components (marked by primes “ $r$ ”). Note that  $q_{\alpha}^{\circ} = q\delta_{1\alpha}$ . Using the components  $q_{\alpha}^{\circ}$  and  $u_{\alpha}^{\circ}(\mathbf{q})$  we obtain (as before) the strain tensor  $\varepsilon_{\alpha\beta}^{\circ}(\mathbf{q})$  in NRC. Importantly,  $\varepsilon_{22}^{\circ}(\mathbf{q}) = 0$  since  $q_2^{\circ} = 0$ , cf. Eq. (E7). We thus only have two independent components of the strain tensor field in NRC. We alternatively write for later convenience  $u_L(\mathbf{q}) \equiv u_1^{\circ}(\mathbf{q})$ ,  $u_T(\mathbf{q}) \equiv u_2^{\circ}(\mathbf{q})$ ,  $\varepsilon_L(\mathbf{q}) \equiv \varepsilon_{11}^{\circ}(\mathbf{q})$  and  $\varepsilon_T(\mathbf{q}) \equiv \varepsilon_{12}^{\circ}(\mathbf{q}) \equiv \varepsilon_{21}^{\circ}(\mathbf{q})$  for the longitudinal and transverse components of the displacement and strain tensor fields in NRC. Note that  $\varepsilon_L(\mathbf{q}) = iqu_L(\mathbf{q})$  and  $\varepsilon_T(\mathbf{q}) = iqu_T(\mathbf{q})/2$ , i.e. displacement and strain fields in NRC contain essentially the same information.

*Correlation functions in NRC.* The correlation functions  $c_{\alpha\beta\gamma\delta}^{\circ}(\mathbf{q}) \equiv \langle \varepsilon_{\alpha\beta}^{\circ}(\mathbf{q}) \varepsilon_{\gamma\delta}^{\circ}(-\mathbf{q}) \rangle$  may for *finite*  $N_c$  not only depend on  $q$  but also on  $\hat{\mathbf{q}}$ . Consistently with Eq. (A20) and Refs. [16, 17, 19] we thus operationally define the ICFs  $c_L(q) \equiv \langle c_{1111}^{\circ}(\mathbf{q}) \rangle_{\hat{\mathbf{q}}}$ ,  $c_T(q) \equiv \langle c_{1212}^{\circ}(\mathbf{q}) \rangle_{\hat{\mathbf{q}}}$ ,  $c_2(q) \equiv \langle c_{2222}^{\circ}(\mathbf{q}) \rangle_{\hat{\mathbf{q}}}$  and  $c_{\perp}(q) \equiv \langle c_{1122}^{\circ}(\mathbf{q}) \rangle_{\hat{\mathbf{q}}}$  by averaging over all wavevectors with  $|\mathbf{q}| \approx q$ . Obviously,

$$c_{2222}^{\circ}(\mathbf{q}) = c_{1122}^{\circ}(\mathbf{q}) = c_2(q) = c_{\perp}(q) = 0 \text{ for } \forall \mathbf{q} \quad (3)$$

since  $\varepsilon_{22}^{\circ}(\mathbf{q}) \propto q_2^{\circ} = 0$ .  $c_L(q)$  and  $c_T(q)$  are called, respectively, the “longitudinal ICF” and the “transverse ICF”.

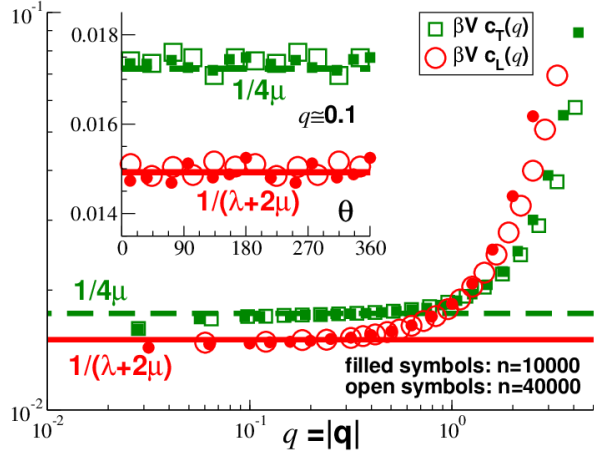


FIG. 2: Rescaled correlation functions in NRC and reciprocal space. The bold dashed and solid lines indicate the expected low- $q$  limit Eq. (4). Inset:  $\beta V c_{1212}^o(\mathbf{q})$  and  $\beta V c_{1111}^o(\mathbf{q})$  vs.  $\theta$  for  $q \approx 0.1$ . Main panel: Semi-logarithmic representation of ICFs  $\beta V c_T(q)$  and  $\beta V c_L(q)$  vs.  $q$ .

According to the equipartition theorem it is well known [6] that

$$\beta V c_L(q) \rightarrow \frac{1}{\lambda + 2\mu} \text{ and } \beta V c_T(q) \rightarrow \frac{1}{4\mu} \text{ for } q \rightarrow 0 \quad (4)$$

and sufficiently large systems. See Appendices E 3 and E 4 for a reminder.

*Measured ICFs.* We turn now to the numerical results of this work. Figure 2 focuses on the two non-vanishing correlation functions obtained in reciprocal space and NRC. All correlation functions are rescaled by  $\beta V$  having thus the dimension of an inverse modulus. As can be seen for the two indicated particle numbers  $n$ , a data collapse for different system sizes is observed, confirming the expected volume scaling. The inset presents the (not yet spherically averaged) correlation functions  $\beta V c_{1212}^o(\mathbf{q})$  and  $\beta V c_{1111}^o(\mathbf{q})$  as functions of the wavevector angle  $\theta$  for one small wavevector with  $q \approx 0.1$ . As expected for isotropic systems, these correlation functions are  $\theta$ -independent (apart from a small noise contribution due to the finite number  $N_c$  of independent configurations). The main panel presents the  $\hat{\mathbf{q}}$ -averaged longitudinal and transverse ICFs  $\beta V c_L(q)$  and  $\beta V c_T(q)$  as functions of  $q$ . The expected large-wavelength limit Eq. (4) is indicated in both panels by bold horizontal lines. As can be seen in the main panel, it is well confirmed for  $q \ll 1$  over at least one order of magnitude. We have used here the known macroscopic Lamé coefficients  $\lambda$  and  $\mu$ . We remind that Eq. (4) has been used in various experimental and numerical studies [9, 10, 21] to fit  $\lambda$  and  $\mu$ .  $c_L(q)$  and  $c_T(q)$  characterize the typical length of the complex random variables  $\varepsilon_L(\mathbf{q})$  and  $\varepsilon_T(\mathbf{q})$ . We note finally that the increase of the ICFs from the low- $q$  asymptotics visible for  $q > 1$  correlates with the deviation of the total static structure factor  $S(q)$  from its low- $q$  plateau (cf. Fig. 6).

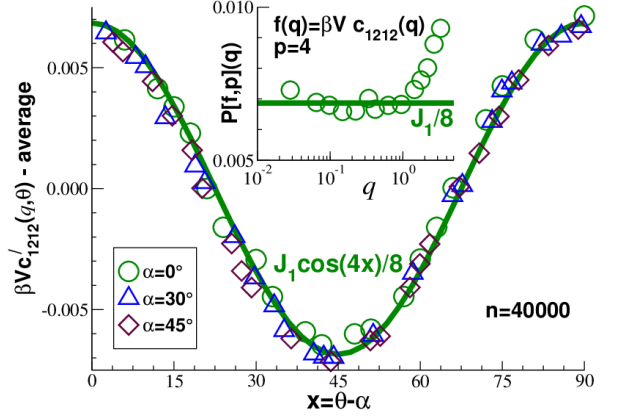


FIG. 3: Rescaled shear-strain correlation function  $f(\mathbf{q}) = \beta V c'_{1212}(\mathbf{q})$  for  $n = 40000$ . Main panel: Angle dependence of vertically shifted  $f(\mathbf{q})$  for  $q \approx 0.1$ . Data collapse is observed using the reduced angle  $x = \theta - \alpha$ . The bold solid line indicates the prediction, Eq. (5). Inset: Comparison of  $P[f, p](q)$  for  $p = 4$  with the predicted low- $q$  limit  $J_1/8$  (bold solid line).

*Correlation functions in reciprocal space.* While remaining in reciprocal space we consider next coordinate frames which are either unrotated ( $\alpha = 0$ ) or rotated as in Fig. 1(b) using the *same* angle  $\alpha$  for all  $\mathbf{q}$ . As reminded above, Eq. (2), the correlation functions  $c_{\alpha\beta\gamma\delta}(\mathbf{q})$  of isotropic achiral systems in two dimensions depend quite generally on the four ICFs  $c_L(q)$ ,  $c_T(q)$ ,  $c_2(q)$  and  $c_\perp(q)$ . According to Eq. (3), the last two of these ICFs must vanish for strain correlation functions while the longitudinal and transverse ICFs,  $c_L(q)$  and  $c_T(q)$ , are given in the low- $q$  limit by Eq. (4). Let us introduce for later convenience the two constants  $J_1 = 1/\mu - 1/(\lambda + 2\mu)$  and  $J_2 = 2/(\lambda + 2\mu)$ . This yields in the original coordinates

$$\beta V c_{1212}(\mathbf{q}) \rightarrow \frac{J_1}{8} \cos(4\theta) + \dots \quad (5)$$

$$\beta V c_{1122}(\mathbf{q}) \rightarrow \frac{J_1}{8} \cos(4\theta) + \dots \quad (6)$$

$$-\frac{\beta V}{2} (c_{1111}(\mathbf{q}) + c_{2222}(\mathbf{q})) \rightarrow \frac{J_1}{8} \cos(4\theta) + \dots \quad (7)$$

$$\frac{\beta V}{2} (c_{1111}(\mathbf{q}) - c_{2222}(\mathbf{q})) \rightarrow \frac{J_2}{4} \cos(2\theta) \quad (8)$$

for  $q \rightarrow 0$ . The dots mark irrelevant constant contributions. See Appendix F for more details. For correlation functions  $c'_{\alpha\beta\gamma\delta}(\mathbf{q})$  in rotated coordinate systems one merely needs to substitute  $\theta$  by  $x = \theta - \alpha$ , cf. Eq. (1).

These relations are put to a test in Fig. 3 where we focus for clarity on the reduced shear-strain autocorrelation function  $f(\mathbf{q}) = \beta V c'_{1212}(\mathbf{q})$  for  $n = 40000$ . The angular dependences are presented in the main panel for one wavevector in the low- $q$  limit. Focusing on the first term in Eq. (5) we have taken off the mean constant average over all  $\theta$  (corresponding to the dots). Importantly, all data for different  $\alpha$  are seen to collapse when plotted as a function of the scaling variable  $x$ . Obviously, this simple scaling (without any characteristic angle) would

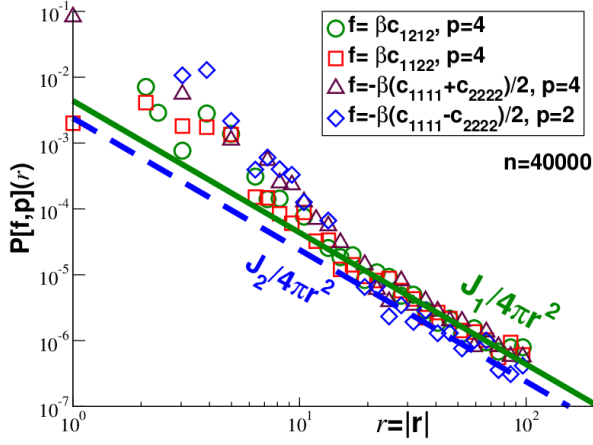


FIG. 4:  $P[f, p](r)$  for various correlation functions and modes  $p$  for  $n = 40000$ . The bold solid line marks the prediction  $J_1/4\pi r^2$  for the first three cases, the dashed line the prediction  $J_2/4\pi r^2$  for the last one.

not hold for anisotropic systems in general. To obtain a precise test of the  $q$ -dependence of  $c_{\alpha\beta\gamma\delta}(\mathbf{q})$  we project out the angular dependences using

$$P[f, p](q) \equiv 2 \times \frac{1}{2\pi} \int_0^{2\pi} d\theta f(q, \theta) \cos(p\theta) \quad (9)$$

for  $p = 2$  and  $p = 4$ . For convenience the prefactor of the integral is chosen such that  $P[\cos(2\theta), 2] = P[\cos(4\theta), 4] = 1$ . The result for the shear-stress autocorrelation function with  $p = 4$  is shown in the inset of Fig. 3. In agreement with Eq. (5) the presented data is given by  $J_1/8$  (solid line) for sufficiently small wavevectors. Equivalent results have been obtained for the other correlation functions mentioned above.

*Real space correlation functions.* Finally, we turn to the correlation functions  $c'_{\alpha\beta\gamma\delta}(\mathbf{r}) = \mathcal{F}^{-1}[c'_{\alpha\beta\gamma\delta}(\mathbf{q})]$  in real space. As shown in Appendix F, inverse Fourier transformation implies

$$\beta c'_{1212}(\mathbf{r}) \simeq \frac{J_1}{4\pi r^2} \cos(4x) \text{ for } r \gg 1 \quad (10)$$

with  $x = \theta - \alpha$  being the difference of the angles  $\theta$  and  $\alpha$  indicated in Fig. 1. The same large- $r$  limit holds also for  $\beta c'_{1122}(\mathbf{r})$  and for  $-\beta(c'_{1111}(\mathbf{r}) + c'_{2222}(\mathbf{r}))/2$ . Moreover,

$$\beta(c'_{1111}(\mathbf{r}) - c'_{2222}(\mathbf{r}))/2 \simeq -\frac{J_2}{4\pi r^2} \cos(2x) \quad (11)$$

for  $r \gg 1$ , i.e. a bi-polar symmetry is expected.

The angle dependence for the shear-strain autocorrelation function in real space is presented in Appendix F. A verification of the  $r$ -dependence is obtained using again (now in real space) the projection  $P[f, p](r)$ , cf. Eq. (9). Focusing on  $n = 40000$  several rescaled correlation functions  $f(\mathbf{r})$  are presented in Fig. 4. In agreement with Eq. (10) the indicated first three cases collapse for  $p = 4$

and  $r \gtrsim 20$  on  $J_1/4\pi r^2$  (bold solid line). This confirms the octupolar symmetry of these correlation functions. Confirming Eq. (11) the last case with  $f(\mathbf{r}) = -\beta(c_{1111}(\mathbf{r}) - c_{2222}(\mathbf{r}))/2$  collapses onto  $J_2/4\pi r^2$  (dashed line).  $p = 2$  is used here in agreement with the predicted quadrupolar symmetry of this correlation function. Similar results are obtained for other particle numbers  $n$ . The above findings may be used to compute the linear strain response in real space due to an applied perturbation as discussed in Appendix G.

*Summary.* We have investigated in the present work correlation functions of components of strain tensor fields in two-dimensional, isotropic and achiral elastic bodies. This was done theoretically using the general mathematical structure of isotropic tensor fields (cf. Appendix A 5) and the equipartition theorem of statistical physics applied to strain fluctuations in reciprocal space using NRC (cf. Appendices E 3 and E 4). Numerically we have tested our predictions by means of glass-forming particles deep in the glass regime. This shows that these correlation functions may depend on the coordinates of the field variable ( $q_\alpha$  in reciprocal space or  $r_\alpha$  in real space) and implies in turn that they depend in general on the direction of the field vector and on the orientation of the coordinate system. Scaling with  $x = \theta - \alpha$  these angular dependencies are distinct from those of ordinary anisotropic systems. Importantly, correlation functions of strain tensor fields are components of an isotropic fourth-order tensor field, Eq. (2), being characterized by the two ICFs  $c_L(q)$  and  $c_T(q)$ . Fortunately,  $c_L(q)$  and  $c_T(q)$  are known from the equipartition theorem to become constant in the low- $q$  limit (cf. Appendix E 4). With the asymptotic plateau values being given by the macroscopic Lamé coefficients  $\lambda$  and  $\mu$ , Eq. (4), all strain correlation functions are determined and all (finite) real-space strain correlations must be long-ranged decaying as  $1/r^2$  (cf. Fig. 4). We thus obtain similar results as in our recent study on correlation functions of stress tensor fields [19] (where time-averaged stress fields have been probed while correlations of instantaneous strain fields without time shifts have been considered in the present study). Our numerical findings do agree with other studies of strain correlations [28, 29] being, however, now traced back to the system isotropy and the tensor field nature of the probed correlations. Importantly, we have given here a complete and asymptotically exact description for the correlation functions of strain tensor fields of isotropic elastic bodies. The additional assumption of localized plastic rearrangements (“Eshelbies”) made in several current studies [23, 24, 26, 31] thus appears to be unnecessary [44].

*Outlook.* As shown in Appendix E 4, the static longitudinal and transverse moduli  $L(q)$  and  $G(q)$  in reciprocal space may be obtained quite generally from the ICFs  $c_L(q)$  and  $c_T(q)$ . As will be investigated in future work,  $L(q)$  and  $G(q)$  thus strongly decrease above  $q \approx 1$  showing minima around the main peak of the static structure factor  $S(q)$  [42]. A further generalization of the current work concerns time-dependent correlation func-

tions  $c_{\alpha\beta\gamma\delta}(\mathbf{q}, t) = \langle \varepsilon_{\alpha\beta}(\mathbf{q}, t) \varepsilon_{\alpha\beta}(-\mathbf{q}, t = 0) \rangle$ . These can be again expressed via Eq. (2) in terms of (now time-dependent) longitudinal and transverse ICFs  $c_L(q, t)$  and  $c_T(q, t)$  which are in turn given by time-dependent response functions [16]. Shear-strain correlation functions  $c_{1212}(\mathbf{q}, t)$  must thus reveal octupolar pattern whenever  $|4c_T(q, t) - c_L(q, t)|$  becomes large. Since this term must also become  $q$ -independent in the small- $q$  limit a long-range  $1/r^2$ -decay is then expected for all  $c_{\alpha\beta\gamma\delta}(\mathbf{r}, t)$ .

*Acknowledgments.* We are indebted to the University of Strasbourg for computational resources.

## Appendix A: Isotropic tensors and tensor fields

### 1. Introduction

Familiarity with the general ideas and notations of tensor algebra and analysis [1–5, 8] is taken for granted. A tensor field assigns a tensor to each point of the mathematical space, in our case a  $d$ -dimensional Euclidean vector space [3]. An element of this vector space is denoted by the “spatial position”  $\mathbf{r}$  (real space) or by the “wavevector”  $\mathbf{q}$  for the corresponding Fourier transformed reciprocal space. The relations for tensor fields are formulated below in reciprocal space since this is more convenient both on theoretical and numerical grounds due to the assumed spatial homogeneity (“translational invariance”). The corresponding real space tensor field is finally obtained by inverse Fourier transform. For simplicity we assume Cartesian coordinates with an orthonormal basis  $\{\mathbf{e}_1, \dots, \mathbf{e}_d\}$  [1, 3, 8]. Greek letters  $\alpha, \beta, \dots$  are used for the indices of the tensor (field) components. A twice repeated index  $\alpha$  is summed over the values  $1, \dots, d$ , e.g.,  $\mathbf{q} = q_\alpha \mathbf{e}_\alpha$  with  $q_\alpha$  standing for the vector coordinates. This work is chiefly concerned with tensors  $\mathbf{T}^{(o)} = T_{\alpha_1 \dots \alpha_o} \mathbf{e}_{\alpha_1} \dots \mathbf{e}_{\alpha_o}$  of “order”  $o = 2$  and  $o = 4$  and their corresponding tensor fields with components depending either on  $\mathbf{r}$  or  $\mathbf{q}$ . The order of a component is given by the number of indices. Note that

$$T_{\alpha_1 \dots \alpha_o}(\mathbf{q}) = \mathcal{F}[T_{\alpha_1 \dots \alpha_o}(\mathbf{r})] \quad (\text{A1})$$

for the  $d^o$  coordinates in real and reciprocal space (with  $\mathcal{F}[\dots]$  denoting the Fourier transform as discussed in Appendix B). We consider linear orthogonal coordinate transformations (marked by “\*”)  $\mathbf{e}_\alpha^* = c_{\alpha\beta} \mathbf{e}_\beta$  with matrix coefficients  $c_{\alpha\beta}$  given by the direction cosine  $c_{\alpha\beta} \equiv \cos(\mathbf{e}_\alpha^*, \mathbf{e}_\beta)$  [3].  $c_{\alpha\beta} = \delta_{\alpha\beta}$  if nothing is changed. A simple reflection of, say, the 1-axis corresponds to  $c_{1\beta} = -\delta_{1\beta}$  and  $c_{\alpha\beta} = \delta_{\alpha\beta}$  for  $\alpha \neq 1$ , a rotation in the 12-plane by an angle  $\alpha$  to  $c_{11} = c_{22} = \cos(\alpha)$ ,  $c_{12} = -c_{21} = \sin(\alpha)$  and  $c_{\alpha\beta} = \delta_{\alpha\beta}$  for all other indices. We remind that [3]

$$T_{\alpha_1 \dots \alpha_o}^*(\mathbf{q}) = c_{\alpha_1 \nu_1} \dots c_{\alpha_o \nu_o} T_{\nu_1 \dots \nu_o}(\mathbf{q}) \quad (\text{A2})$$

under a general orthogonal transform. For a reflection of the 1-axis we thus have, e.g.,

$$\begin{aligned} T_{12}^*(\mathbf{q}) &= -T_{12}(\mathbf{q}), T_{11}^*(\mathbf{q}) = T_{11}(\mathbf{q}), \\ T_{1222}^*(\mathbf{q}) &= -T_{1222}(\mathbf{q}), T_{1221}^*(\mathbf{q}) = T_{1221}(\mathbf{q}), \end{aligned} \quad (\text{A3})$$

i.e. we have sign inversion for an *odd number* of indices  $\alpha, \beta, \dots$  equal to the index of the inverted axis. The field vector  $\mathbf{q} = q_\alpha \mathbf{e}_\alpha = q_\alpha^* \mathbf{e}_\alpha^*$  remains unchanged by these “passive” transforms albeit its coordinates change.

### 2. Definitions, properties and construction of general isotropic tensors and tensor fields

*Isotropic tensors.* Isotropic systems are described by “isotropic tensors” and “isotropic tensor fields”. Components of an isotropic tensor remain unchanged by *any* orthogonal coordinate transformation [3, 8], i.e.

$$T_{\alpha_1 \dots \alpha_o}^* = T_{\alpha_1 \dots \alpha_o}. \quad (\text{A4})$$

As noted at the end of Sec. A1 the sign of tensor components change for a reflection at one axis if the number of indices equal to the inverted axis is *odd*. Consistency with Eq. (A4) implies that *all tensor components with an odd number of equal indices must vanish*, e.g.,

$$T_{12} = T_{1112} = T_{1222} = T_{1234} = T_{1344} = 0. \quad (\text{A5})$$

*Isotropic tensor fields.* The corresponding isotropy condition for tensor fields is given by [3]

$$T_{\alpha_1 \dots \alpha_o}^*(q_1, \dots, q_d) = T_{\alpha_1 \dots \alpha_o}(q_1^*, \dots, q_d^*) \quad (\text{A6})$$

with  $q_\alpha^* = c_{\alpha\beta} q_\beta$  which reduces to Eq. (A4) for  $\mathbf{q} = \mathbf{0}$ . Please note that the fields on the left handside of Eq. (A6) are evaluated with the original coordinates of the vector field variable  $\mathbf{q}$  while the fields on the right handside are evaluated with the transformed coordinates. Another way to state this is to say that the left hand fields are computed at the original vector  $\mathbf{q} = (q_1, \dots, q_d)$  while the right hand fields are computed at the “actively transformed” vector  $\mathbf{q}^* = (q_1^*, \dots, q_d^*)$ . It is for this reason that Eq. (A5) does not hold in general for tensor fields, i.e. finite components with an odd number of equal indices, e.g.,  $T_{1222}(\mathbf{q}) \neq 0$ , are possible in principle for finite  $\mathbf{q}$ .

*Natural Rotated Coordinates.* Fortunately, there is a convenient coordinate system where the nice symmetry Eq. (A5) for isotropic tensors can be also used for isotropic tensor fields. In these “Natural Rotated Coordinates” (NRC) the coordinate system for *each* wavevector  $\mathbf{q}$  is rotated until the 1-axis coincides with the  $\mathbf{q}$ -direction, i.e.  $q_\alpha^\circ = q \delta_{1\alpha}$  with  $q = |\mathbf{q}|$ . These tensor field components in NRC are marked by “o” to distinguish them from standard rotated tensor fields (marked by primes “r”) where the *same* rotation is used for all  $\mathbf{q}$ . If in addition  $T_{\alpha_1 \dots \alpha_o}^\circ(\mathbf{q})$  is an *even* function of its field variable  $\mathbf{q}$  (as in the case of achiral systems for even order  $o$ ) it can be shown [19] that all tensor field components with an odd number of equal indices must vanish.



*Product theorem for isotropic tensor fields.* Let us state a useful theorem for a general tensor field  $\mathbf{C}(\mathbf{q}) = \mathbf{A}(\mathbf{q}) \otimes \mathbf{B}(\mathbf{q})$  with  $\mathbf{A}(\mathbf{q})$  and  $\mathbf{B}(\mathbf{q})$  being two isotropic tensor fields and  $\otimes$  standing either for an outer product, e.g.  $C_{\alpha\beta\gamma\delta}(\mathbf{q}) = A_{\alpha\beta}(\mathbf{q})B_{\gamma\delta}(\mathbf{q})$ , or an inner product, e.g.  $C_{\alpha\beta\gamma\delta}(\mathbf{q}) = A_{\alpha\beta\gamma\nu}(\mathbf{q})B_{\nu\delta}(\mathbf{q})$ . Hence,

$$\begin{aligned} \mathbf{C}^*(\mathbf{q}) &= (\mathbf{A}(\mathbf{q}) \otimes \mathbf{B}(\mathbf{q}))^* = \mathbf{A}^*(\mathbf{q}) \otimes \mathbf{B}^*(\mathbf{q}) \\ &= \mathbf{A}(\mathbf{q}^*) \otimes \mathbf{B}(\mathbf{q}^*) = \mathbf{C}(\mathbf{q}^*) \end{aligned} \quad (\text{A7})$$

using in the second step a general property of tensor (field) products, due to Eq. (A2), and in the third step Eq. (A6) for the fields  $\mathbf{A}(\mathbf{q})$  and  $\mathbf{B}(\mathbf{q})$  where  $\mathbf{q}^*$  stands for the “actively” transformed field variable. We have thus demonstrated that  $\mathbf{C}(\mathbf{q})$  is also an isotropic tensor field. This theorem allows to construct isotropic tensor fields from known isotropic tensor fields  $\mathbf{A}(\mathbf{q})$  and  $\mathbf{B}(\mathbf{q})$ .

*Multilinear forms.* Isotropic tensor fields may be also constructed using multilinear forms [3, 8, 19]

$$\mathcal{L}(\mathbf{v}^1, \dots, \mathbf{v}^o; \mathbf{q}) = T_{\alpha_1 \dots \alpha_o}(\mathbf{q}) v_{\alpha_1}^1 \dots v_{\alpha_o}^o \quad (\text{A8})$$

of order  $o$  where  $\mathcal{L}$  stands for a linear and (first order) homogeneous functional of a  $d$ -dimensional vector space [3, 8] and  $\mathbf{v}^1, \dots, \mathbf{v}^o$  are  $o$  arbitrary vectors (with superscripts for the numbering of these vectors). For tensor fields  $\mathcal{L}$  also depends on  $\mathbf{q}$ . The goal is then to construct generic isotropic tensor fields associated with multilinear forms. This is done in a first step by means of additive terms of all possible scalars formed with the vectors  $\mathbf{v}^1, \dots, \mathbf{v}^o$  and  $\mathbf{q}$ , e.g., inner products  $\mathbf{v}^1 \cdot \mathbf{v}^2$ ,  $\mathbf{v}^1 \cdot \mathbf{q}$  or  $\mathbf{q} \cdot \mathbf{q}$  or triple products such as  $[\mathbf{v}^1 \mathbf{v}^2 \mathbf{q}]$ . In a second step all terms are eliminated which are incompatible with Eq. (A6) and other imposed symmetries.

*Kronecker and Levi-Civita tensors.* We remind that the Kronecker symbol  $\delta_{\alpha\beta}$  is an invariant tensor,  $\delta_{\alpha\beta}^* = \delta_{\alpha\beta}$  [3]. As a consequence, any tensor field, only containing additive terms  $i(q)\delta_{\alpha\beta}\delta_{\gamma\delta}$  with  $i(q)$  being an invariant scalar, is an isotropic tensor field. The same applies for tensor fields with terms containing factors of  $\hat{q}_\alpha = \hat{\mathbf{q}} \cdot \mathbf{e}_\alpha$  since using Eq. (A6) and Eq. (A2) this implies, e.g.,

$$(i(q)\hat{q}_\alpha\hat{q}_\beta\delta_{\gamma\delta})^* = i(q)\hat{q}_\alpha^*\hat{q}_\beta^*\delta_{\gamma\delta}. \quad (\text{A9})$$

As discussed elsewhere [3, 19, 34], the isotropy condition becomes more severe for terms containing the Levi-Civita tensor  $\epsilon_{\alpha\beta\gamma}$  [1] which is only invariant for the rotation subgroup but not for reflections. However, such terms are irrelevant for achiral systems [19].

### 3. Summary of assumed symmetries

All second-order tensors in this work are symmetric,  $T_{\alpha\beta} = T_{\beta\alpha}$ , and the same applies for the corresponding tensor fields in either  $\mathbf{r}$ - or  $\mathbf{q}$ -space. This is, e.g., the case for the strain field  $\epsilon_{\alpha\beta}(\mathbf{q}) = \mathcal{F}[\epsilon_{\alpha\beta}(\mathbf{r})]$ . We assume for

all forth-order tensor fields that

$$T_{\alpha\beta\gamma\delta}(\mathbf{q}) = T_{\beta\alpha\gamma\delta}(\mathbf{q}) = T_{\alpha\beta\delta\gamma}(\mathbf{q}) \quad (\text{A10})$$

$$T_{\alpha\beta\gamma\delta}(\mathbf{q}) = T_{\gamma\delta\alpha\beta}(\mathbf{q}) \text{ and} \quad (\text{A11})$$

$$T_{\alpha\beta\gamma\delta}(\mathbf{q}) = T_{\alpha\beta\gamma\delta}(-\mathbf{q}). \quad (\text{A12})$$

Let us remind that forth-order tensor fields are often constructed by taking outer products [8] of second-order tensor fields. We consider, e.g., correlation functions  $\langle \hat{T}_{\alpha\beta}(\mathbf{q})\hat{T}_{\gamma\delta}(-\mathbf{q}) \rangle$  with  $\hat{T}_{\alpha\beta}(\mathbf{q})$  being an instantaneous (not ensemble-averaged) second-order tensor field. Eq. (A10) then follows from the symmetry of the second-order tensor fields. The evenness of forth-order tensor fields, Eq. (A12), is a necessary condition for *achiral* systems. It implies that  $T_{\alpha\beta\gamma\delta}(\mathbf{q})$  is real if  $T_{\alpha\beta\gamma\delta}(\mathbf{r})$  is real and, moreover, Eq. (A11) for correlation functions since  $\langle \hat{T}_{\alpha\beta}(\mathbf{q})\hat{T}_{\gamma\delta}(-\mathbf{q}) \rangle = \langle \hat{T}_{\gamma\delta}(\mathbf{q})\hat{T}_{\alpha\beta}(-\mathbf{q}) \rangle$ . As already emphasized, it is assumed that all our systems are *isotropic*, i.e., Eq. (A6) must hold for the ensemble-averaged tensor fields. Since our systems are also *achiral*, tensor field components computed in NRC with an odd number of equal indices must vanish.

## 4. Isotropic tensors

Isotropic tensors of different order are discussed, e.g., in Sec. 2.5.6 of Ref. [8]. Due to Eq. (A5) all such tensors of odd order must vanish. The finite isotropic tensors of lowest order are thus

$$T_{\alpha\beta} = k_1\delta_{\alpha\beta}, \quad (\text{A13})$$

$$T_{\alpha\beta\gamma\delta} = i_1\delta_{\alpha\beta}\delta_{\gamma\delta} + i_2(\delta_{\alpha\gamma}\delta_{\beta\delta} + \delta_{\alpha\delta}\delta_{\beta\gamma}) \quad (\text{A14})$$

where  $k_1$ ,  $i_1$  and  $i_2$  are invariant scalars. Please note that all symmetries stated above hold, especially also Eq. (A5). Note that the symmetry Eq. (A10) was used for the second relation, Eq. (A14). Importantly, this implies that only *two* coefficients are needed for a forth-order isotropic tensor. As a consequence, the elastic modulus tensor  $E_{\alpha\beta\gamma\delta}$  is completely described by *two* elastic moduli, say  $\lambda$  and  $\mu$  (cf. Sec. D).

## 5. Tensor fields for isotropic achiral systems

With  $l_n(q)$ ,  $k_n(q)$ ,  $j_n(q)$  and  $i_n(q)$  being invariant scalar functions the most general isotropic tensor fields for  $1 \leq o \leq 4$  compatible with the assumed symmetries

(cf. Sec. A 3) are given by [3, 19].

$$T_\alpha(\mathbf{q}) = l_1(q) q_\alpha \quad (\text{A15})$$

$$T_{\alpha\beta}(\mathbf{q}) = k_1(q) \delta_{\alpha\beta} + k_2(q) q_\alpha q_\beta \quad (\text{A16})$$

$$T_{\alpha\beta\gamma}(\mathbf{q}) = j_1(q) q_\alpha \delta_{\beta\gamma} + j_2(q) q_\beta \delta_{\alpha\gamma} + j_3(q) q_\gamma \delta_{\alpha\beta} + j_4(q) q_\alpha q_\beta q_\gamma \quad (\text{A17})$$

$$T_{\alpha\beta\gamma\delta}(\mathbf{q}) = i_1(q) \delta_{\alpha\beta} \delta_{\gamma\delta} + i_2(q) (\delta_{\alpha\gamma} \delta_{\beta\delta} + \delta_{\alpha\delta} \delta_{\beta\gamma}) + i_3(q) (q_\alpha q_\beta \delta_{\gamma\delta} + q_\gamma q_\delta \delta_{\alpha\beta}) + i_4(q) q_\alpha q_\beta q_\gamma q_\delta + i_5(q) (q_\alpha q_\gamma \delta_{\beta\delta} + q_\alpha q_\delta \delta_{\beta\gamma} + q_\beta q_\gamma \delta_{\alpha\delta} + q_\beta q_\delta \delta_{\alpha\gamma}). \quad (\text{A18})$$

Let us check that the stated relations are reasonable. All relations reduce (continuously) for  $\mathbf{q} \rightarrow \mathbf{0}$  to the isotropic tensors stated in Sec. A 4; all are, according to the discussion in the last paragraph of Sec. A 2, isotropic tensor fields consistent with Eq. (A6) and all symmetries stated in Sec. A 3 for the second- and forth-order tensor fields are satisfied. All tensor fields of even (odd) order are even (odd) with respect to  $\mathbf{q}$ . Hence, tensor fields of odd order vanish for  $\mathbf{q} \rightarrow \mathbf{0}$ . Terms due to the invariants  $k_1(q)$ ,  $i_1(q)$  and  $i_2(q)$  are independent of the coordinate system. All other terms depend on the components  $q_\alpha$ .

For finite wavevectors it is useful to rewrite the forth-order tensor field Eq. (A18) in terms of the components  $\hat{q}_\alpha$  of the normalized wavevector  $\hat{\mathbf{q}}$  and to redefine  $i_3(q) \rightarrow i_3(q)/q^2$ ,  $i_4(q) \rightarrow i_4(q)/q^4$  and  $i_5(q) \rightarrow i_5(q)/q^2$ . We thus rewrite Eq. (A18) as

$$T_{\alpha\beta\gamma\delta}(\mathbf{q}) = i_1(q) \delta_{\alpha\beta} \delta_{\gamma\delta} + i_2(q) [\delta_{\alpha\gamma} \delta_{\beta\delta} + \delta_{\alpha\delta} \delta_{\beta\gamma}] + i_3(q) [\hat{q}_\alpha \hat{q}_\beta \delta_{\gamma\delta} + \hat{q}_\gamma \hat{q}_\delta \delta_{\alpha\beta}] + i_4(q) \hat{q}_\alpha \hat{q}_\beta \hat{q}_\gamma \hat{q}_\delta + i_5(q) [\hat{q}_\alpha \hat{q}_\gamma \delta_{\beta\delta} + \hat{q}_\alpha \hat{q}_\delta \delta_{\beta\gamma} + \hat{q}_\beta \hat{q}_\gamma \delta_{\alpha\delta} + \hat{q}_\beta \hat{q}_\delta \delta_{\alpha\gamma}]. \quad (\text{A19})$$

Now all  $i_n(q)$  have the same physical units. Fortunately, in many physical systems the (redefined) invariants  $i_n(q)$  become constant or negligible for sufficiently small  $q$ .

## 6. Forth-order tensor fields in two dimensions

For the two-dimensional systems studied numerically in this work it can be shown [16, 19] that the last contribution to the general forth-order tensor field, Eq. (A19), is not needed, i.e.  $i_5(q) = 0$ . To see this let us consider the tensor field in NRC. We define the four functions

$$\left. \begin{aligned} c_L(q) &\equiv T_{1111}^\circ(\mathbf{q}) \\ c_T(q) &\equiv T_{1212}^\circ(\mathbf{q}) \\ c_2(q) &\equiv T_{2222}^\circ(\mathbf{q}) \\ c_\perp(q) &\equiv T_{1122}^\circ(\mathbf{q}) \end{aligned} \right\} \text{ for } q_\alpha^\circ = q \delta_{1\alpha}. \quad (\text{A20})$$

For an isotropic system these four functions can only depend on the wavenumber  $q$  but not on the direction  $\hat{\mathbf{q}}$  of

the wavevector  $\mathbf{q}$ . (For real physical systems there may always be some noise. For this reason we have introduced these invariants in the main part using an additional  $\hat{\mathbf{q}}$ -averaging.) Importantly, all other components  $T_{\alpha\beta\gamma\delta}^\circ(\mathbf{q})$  are either by Eq. (A10) and Eq. (A11) identical to these invariants or must vanish for an odd number of equal indices as reminded in Sec. A 2. The  $d^4 = 16$  components  $T_{\alpha\beta\gamma\delta}^\circ(\mathbf{q})$  are thus completely determined by the four invariants and this for any  $\mathbf{q}$ .  $T_{\alpha\beta\gamma\delta}(\mathbf{q})$  is then obtained by the inverse rotation to the original unrotated frame using Eq. (A2). Let us set

$$\begin{aligned} c_L(q) &= i_1(q) + 2i_2(q) + 2i_3(q) + i_4(q) \\ c_2(q) &= i_1(q) + 2i_2(q) \\ c_\perp(q) &= i_1(q) + i_3(q) \\ c_T(q) &= i_2(q) \end{aligned} \quad (\text{A21})$$

being consistent with the inverse relations

$$\begin{aligned} i_1(q) &= c_2(q) - 2c_T(q) \\ i_2(q) &= c_T(q) \\ i_3(q) &= c_\perp(q) - c_2(q) + 2c_T(q) \\ i_4(q) &= c_L(q) + c_2(q) - 2c_\perp(q) - 4c_T(q). \end{aligned} \quad (\text{A22})$$

In agreement with Ref. [16, 19] the inverse rotation back to the original frame leads to Eq. (A19) with  $i_5(q) \equiv 0$ .

We have formulated above all tensor fields in terms of the wavevector  $\mathbf{q}$  and its components since it is most convenient to start the analysis in reciprocal space. The above results also hold, however, in real space. For instance, a forth-order tensor field of an isotropic achiral system in two dimensions must take in real space the general form

$$T_{\alpha\beta\gamma\delta}(\mathbf{r}) = \tilde{i}_1(r) \delta_{\alpha\beta} \delta_{\gamma\delta} + \tilde{i}_2(r) [\delta_{\alpha\gamma} \delta_{\beta\delta} + \delta_{\alpha\delta} \delta_{\beta\gamma}] + \tilde{i}_3(r) [\hat{r}_\alpha \hat{r}_\beta \delta_{\gamma\delta} + \hat{r}_\gamma \hat{r}_\delta \delta_{\alpha\beta}] + \tilde{i}_4(r) \hat{r}_\alpha \hat{r}_\beta \hat{r}_\gamma \hat{r}_\delta \quad \text{for } r > 0 \quad (\text{A23})$$

where the  $\tilde{i}_n(r)$  denote the invariants in real space and  $\hat{r}_\alpha = r_\alpha/r$  a component of the normalized vector  $\hat{\mathbf{r}} = \mathbf{r}/r$ . As already stated, Eq. (A1), the tensor field components in real and reciprocal space are related by Fourier transformation. Note that the  $\tilde{i}_n(r)$  are in general *not* the Fourier transformations of the  $i_n(q)$ . For the important case that the invariants in reciprocal space are  $q$ -independent constants it follows quite generally that

$$\begin{aligned} 4\pi r^2 \tilde{i}_1 &= 4i_3 + 5i_4 \\ 4\pi r^2 \tilde{i}_2 &= -i_4 \\ 4\pi r^2 \tilde{i}_3 &= -4i_3 - 6i_4 \\ 4\pi r^2 \tilde{i}_4 &= 8i_4 \end{aligned} \quad (\text{A24})$$

for  $r > 0$ . (Additional  $\delta(\mathbf{r})$ -terms arise at the origin. The constant invariants  $i_1$  and  $i_2$  only contribute to these terms.) That this holds can be readily shown using relations put forward in Appendix B 3 and Appendix F.

## Appendix B: Fourier transformations

### 1. Continuous Fourier transform

We consider real-valued functions  $f(\mathbf{r})$  in  $d$  dimensions. Following Refs. [17, 19, 45] we define the Fourier transform  $f(\mathbf{q}) = \mathcal{F}[f(\mathbf{r})]$  from “real space” (variable  $\mathbf{r}$ ) to “reciprocal space” (variable  $\mathbf{q}$ ) by

$$f(\mathbf{q}) = \frac{1}{V} \int d\mathbf{r} f(\mathbf{r}) \exp(-i\mathbf{q} \cdot \mathbf{r}) \quad (\text{B1})$$

with  $V$  being the volume of the system. The inverse Fourier transform is then given by

$$f(\mathbf{r}) = \mathcal{F}^{-1}[f(\mathbf{q})] = \frac{V}{(2\pi)^d} \int d\mathbf{q} f(\mathbf{q}) \exp(i\mathbf{q} \cdot \mathbf{r}). \quad (\text{B2})$$

Note that  $f(\mathbf{r})$  and  $f(\mathbf{q})$  have the same dimension. For notational simplicity the function names remain unchanged. We remind the Fourier transforms

$$\mathcal{F} \left[ \frac{\partial}{\partial r_\alpha} f(\mathbf{r}) \right] = i q_\alpha f(\mathbf{q}) \quad (\text{B3})$$

$$\mathcal{F} [\delta(\mathbf{r} - \mathbf{v})] = \frac{1}{V} \exp(-i\mathbf{q} \cdot \mathbf{v}) \quad (\text{B4})$$

with  $\delta(\mathbf{r})$  being Dirac’s delta function. Let us consider the spatial correlation function

$$c(\mathbf{r}) = \frac{1}{V} \int d\mathbf{r}' g(\mathbf{r} + \mathbf{r}') h(\mathbf{r}') \quad (\text{B5})$$

of real-valued fields  $g(\mathbf{r})$  and  $h(\mathbf{r})$ . According to the “correlation theorem” [46] this becomes

$$c(\mathbf{q}) = g(\mathbf{q}) h^*(\mathbf{q}) = g(\mathbf{q}) h(-\mathbf{q}) \quad (\text{B6})$$

in reciprocal space (with  $\star$  marking the conjugate complex). For auto-correlation functions, i.e. for  $g(\mathbf{r}) = h(\mathbf{r})$ , this simplifies to (“Wiener-Khinchin theorem”)

$$c(\mathbf{q}) = g(\mathbf{q}) g^*(\mathbf{q}) = |g(\mathbf{q})|^2, \quad (\text{B7})$$

i.e. the Fourier transformed auto-correlation functions are real and  $\geq 0$  for all  $\mathbf{q}$ . Moreover, we shall consider correlation functions  $c(\mathbf{r})$ , Eq. (B5), being *even* in real space,  $c(\mathbf{r}) = c(-\mathbf{r})$ , and thus also in reciprocal space,  $c(\mathbf{q}) = c(-\mathbf{q}) = c^*(\mathbf{q})$ , i.e.  $c(\mathbf{q})$  is real.

### 2. Discrete Fourier transform on microcell grid

All fields  $f(\mathbf{r})$  are stored on a regular equidistant  $d$ -dimensional grid as shown in Fig. 5 for  $d = 2$ . Periodic boundary conditions are assumed [32]. The discrete Fourier transform and its inverse become

$$f(\mathbf{q}) = \frac{1}{n_V} \sum_{\mathbf{r}} f(\mathbf{r}) \exp(-i\mathbf{q} \cdot \mathbf{r}) \quad (\text{B8})$$

$$f(\mathbf{r}) = \sum_{\mathbf{q}} f(\mathbf{q}) \exp(i\mathbf{q} \cdot \mathbf{r}) \quad (\text{B9})$$

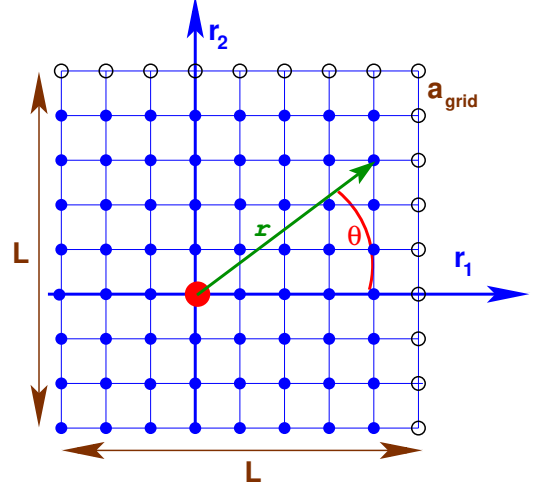


FIG. 5: Two-dimensional ( $d = 2$ ) square lattice with  $a_{\text{grid}}$  being the lattice constant and  $n_L = L/a_{\text{grid}}$  the number of grid points in one spatial dimension. The filled circles indicate microcells of the principal box, the open circles some periodic images. The spatial position  $\mathbf{r}$  of a microcell is either given by the  $r_1$ - and  $r_2$ -coordinates (in the principal box) or by the distance  $r = |\mathbf{r}|$  from the origin (large circle) and the angle  $\theta$ .

with  $\sum_{\mathbf{r}}$  and  $\sum_{\mathbf{q}}$  being discrete sums over  $n_V = n_L^d = V/a_{\text{grid}}^d$  grid points in, respectively, real or reciprocal space. To take advantage of the implemented Fast-Fourier transform (FFT) routines [46] the number of grid points in each spatial direction  $n_L = L/a_{\text{grid}}$  is an integer-power of 2. As shown in Fig. 5 we label the grid points in real and reciprocal space using

$$\frac{r_\alpha}{a_{\text{grid}}} = n_\alpha \text{ and } q_\alpha a_{\text{grid}} = \frac{2\pi}{n_L} n_\alpha \quad (\text{B10})$$

with  $n_\alpha = -n_L/2 + 1, \dots, 0, 1, \dots, n_L/2$ .

### 3. $\mathcal{F}^{-1}[\cos(p\theta_q)]$ and $\mathcal{F}^{-1}[\sin(p\theta_q)]$ for $d = 2$

As discussed in the main part all correlation functions in reciprocal space become in the large-wavelength limit independent of the magnitude  $q$  of the wavevector  $\mathbf{q}$  but depend on its angle  $\theta_q$  (and, more generally, on the angle difference  $\theta_q - \alpha$  for rotated coordinate frames). These angular dependencies can be expressed by sums of the Fourier weights  $\cos(p\theta_q)$  and  $\sin(p\theta_q)$  with  $p$  being an integer. We denote these weights by  $w_p(\theta_q)$ . We thus need to compute the inverse Fourier transforms of  $f(\mathbf{q}) = w_p(\theta_q)/V$ . More specifically, we are interested in modes with  $p = 2$  and  $p = 4$ . Additional constant terms ( $p = 0$ ), such as the ones indicated by dots in Eqs. (5-7), are irrelevant for our considerations, leading merely to



$\delta$ -contributions at  $r = 0$ . For  $d = 2$  Eq. (B2) becomes

$$f(\mathbf{r}) = \frac{1}{4\pi^2} \int_0^\infty dq q \times \int_0^{2\pi} d\theta_q w_p(\theta_q) \exp[iqr \cos(\theta_q - \theta_r)] \quad (\text{B11})$$

with  $\theta_r$  being the angle of  $\hat{\mathbf{r}} = (\cos(\theta_r), \sin(\theta_r))$ . We make now the substitution  $\theta = \theta_q - \theta_r$  and use that [47]

$$\begin{aligned} \cos(p\theta + p\theta_r) + \cos(-p\theta + p\theta_r) &= 2 \cos(p\theta) \cos(p\theta_r) \\ \sin(p\theta + p\theta_r) + \sin(-p\theta + p\theta_r) &= 2 \cos(p\theta) \sin(p\theta_r). \end{aligned}$$

We remind that following Eq. (9.1.21) of Ref. [47] the integer Bessel function  $J_p(z)$  may be written

$$J_p(z) = \frac{i^{-p}}{\pi} \int_0^\pi d\theta \cos(p\theta) \exp[iz \cos(\theta)]. \quad (\text{B12})$$

This leads to

$$f(\mathbf{r}) = \frac{i^p}{2\pi} w_p(\theta_r) \int_0^\infty dq q J_p(rq). \quad (\text{B13})$$

For finite  $r$  we may rewrite this as

$$f(\mathbf{r}) = \frac{i^p p}{2\pi r^2} w_p(\theta_r) \times \lim_{t \rightarrow \infty} I_p(t) \text{ for } r > 0 \quad (\text{B14})$$

where we have set  $I_p(t) \equiv \int_0^t dt' t' J_p(t')/p$ . As may be seen from Eq. (11.4.16) of Ref. [47] the latter integral becomes [48]

$$I_p(t) \rightarrow 1 \text{ for } t \rightarrow \infty \text{ and } p > -2 \quad (\text{B15})$$

from which we obtain the final result

$$f(\mathbf{r}) = \frac{i^p p}{2\pi r^2} w_p(\theta_r) \text{ for } r > 0. \quad (\text{B16})$$

Note that  $f(\mathbf{r}) = f(-\mathbf{r})$  and that  $f(\mathbf{r})$  is real for even  $p$ . Generalizing the above argument it is seen that  $f(\mathbf{r}) \propto 1/r^d$  for higher dimensions  $d$ .

## Appendix C: Computational details

### 1. Simulation model

We consider systems of polydisperse Lennard-Jones (pLJ) particles in  $d = 2$  dimensions where two particles  $i$  and  $j$  of diameter  $D_i$  and  $D_j$  interact by means of a central pair potential [17, 19, 35–38, 42]

$$u(s) = 4\epsilon \left( \frac{1}{s^{12}} - \frac{1}{s^6} \right) \text{ with } s = \frac{r}{(D_i + D_j)/2} \quad (\text{C1})$$

being the reduced distance according to the Lorentz rule [33]. This potential is truncated and shifted [19, 32] with a cutoff  $s_{\text{cut}} = 2s_{\text{min}}$  given by the minimum  $s_{\text{min}}$  of  $u(s)$ . Lennard-Jones units [32] are used throughout this study,

i.e.  $\epsilon = 1$  and the average particle diameter is set to unity. The diameters are uniformly distributed between 0.8 and 1.2. We also set Boltzmann's constant  $k_B = 1$  and assume that all particles have the same mass  $m = 1$ . The last point is irrelevant for the presented Monte Carlo (MC) simulations [32]. Time is measured in units of MC steps (MCS) throughout this work.

### 2. Parameters and configuration ensembles

We focus on systems with  $n = 10000$  and  $n = 40000$  particles. We first equilibrate  $N_c = 200$  independent configurations  $c$  at a high temperature  $T = 0.55$  in the liquid limit. These configurations are adiabatically cooled down using a combination of local MC moves [32] and swap MC moves exchanging the sizes of pairs of particles [37, 43]. In addition, an MC barostat [32] imposes an average normal stress  $P = 2$  [35, 37]. At the working temperature  $T = 0.2$  we first thoroughly temper over  $\Delta\tau = 10^7$  all configurations with switched-on local, swap and barostat MC moves and then again over  $\Delta\tau = 10^7$  with switched-on local and swap moves and switched-off barostat moves. The final production runs are carried out only keeping local MC moves at constant volume  $V$ . Under these conditions,  $T = 0.2$  is well below the glass transition temperature  $T_g \approx 0.26$  determined in previous work [35, 37]. Due to the barostat used for the cooling the box volume  $V = L^d$  differs slightly between different configurations  $c$  while  $V$  is identical for all frames  $t$  of the time-series of the same configuration  $c$ . In all cases the number density is of order unity, i.e. the particle number  $n$  and the volume  $V$  are similar.

### 3. Discrete fields on grid

The different fields considered are stored on equidistant discrete grids as sketched in Fig. 5. The same  $n_L$  is used for both spatial directions and for all configurations and frames of a given particle number  $n$ . As already mentioned, the box volume  $V = L^2$  fluctuates slightly between different configurations  $c$  (at same  $n$ ) due to the barostat used for the cooling, tempering and equilibration of the systems. Accordingly,  $a_{\text{grid}}$  also differs between different configurations  $c$ . These fluctuations become small, however, with increasing system size. If nothing else is mentioned we report data obtained using a lattice constant  $a_{\text{grid}} \approx 0.2$ . As shown in Fig. 6 for the rescaled transverse ICF  $\beta V c_T(q)$  plotted using a double-logarithmic representation, there is no need to further decrease  $a_{\text{grid}}$ . Even the very large grid constant  $a_{\text{grid}} \approx 3.6$  gives, apparently, the correct large-wavelength asymptote  $\beta c_T(q) \approx 1/4\mu$  indicated by the dashed horizontal line. Figure 6 is further discussed in Appendix E 1.

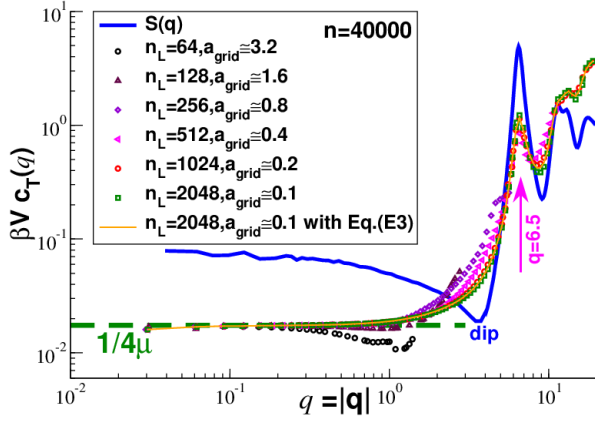


FIG. 6: Rescaled transverse ICF  $\beta V c_T(q)$  for different grid constants  $a_{\text{grid}}$  as indicated. The open symbols have been obtained using Eq. (E2), the thin solid line using Eq. (E3) and  $n_L = 2048$ . Importantly, we obtain the same results in all cases where  $q u_{\text{rms}} \ll 1$  and  $q a_{\text{grid}} \ll 1$ . Even a rather coarse grid, say for  $n_L = 64$ , is sufficient to confirm the expected large-wavelength limit (horizontal dashed line). The total static structure factor  $S(q)$  is shown for comparison (solid line). The “dip” of  $S(q)$  around  $q \approx 4$  is caused by the polydispersity of the particles as emphasized elsewhere [42].  $S(q)$  and  $\beta V c_T(q)$ , at least for sufficiently small  $a_{\text{grid}}$ , have both a strong peak located similarly at  $q \approx 6.5$  (arrow).

#### 4. Data sampling

For each particle number  $n$  and each of the  $N_c$  independent configurations  $c$  we store ensembles of time series containing  $N_t = 10000$  instantaneous “frames”  $t$ . These are obtained using the equidistant time intervals  $\delta\tau = 1000$  for  $n = 10000$  and  $\delta\tau = 100$  for the other system sizes. As described in Appendix E1, we compute for each configuration  $c$  and each particle  $a$  the reference position  $\tilde{\mathbf{r}}_a$ . Using this we obtain for each frame  $t$  the displacement vector  $\mathbf{u}_a(t) = \mathbf{r}_a(t) - \tilde{\mathbf{r}}_a$ . This determines the displacement field  $\mathbf{u}(\mathbf{r})$  according to Eq. (E2). Starting from the displacement field  $\mathbf{u}(\mathbf{r})$  stored on the grid we compute next the Fourier transform  $\mathbf{u}(\mathbf{q})$ . Using the displacement field in reciprocal space we obtain as described in Appendix E2 the strain tensor fields  $\varepsilon_{\alpha\beta}(\mathbf{q})$  in reciprocal space for each  $c$  and  $t$  and from this the correlation functions  $c_{\alpha\beta\gamma\delta}(\mathbf{q}) = \langle \varepsilon_{\alpha\beta}(\mathbf{q}) \varepsilon_{\gamma\delta}(-\mathbf{q}) \rangle$  averaged over all  $c$  and  $t$ . For the reported correlation functions  $c'_{\alpha\beta\gamma\delta}(\mathbf{q}) = \langle \varepsilon'_{\alpha\beta}(\mathbf{q}) \varepsilon'_{\gamma\delta}(-\mathbf{q}) \rangle$  in a coordinate system turned by an angle  $\alpha$  we first compute the new components  $u'_\alpha(\mathbf{r})$  and  $q'_\alpha$  of displacement field and wavevector. (Alternatively, one may also rotate  $\varepsilon_{\gamma\delta}(\mathbf{q})$ .) For the ICFs  $c_L(q)$  and  $c_T(q)$  obtained using NRC we first get the longitudinal and transverse displacement fields  $u_L(\mathbf{q})$  and  $u_T(\mathbf{q})$  in NRC and from those using Eq. (E9) and Eq. (E10) the longitudinal and transverse strains  $\varepsilon_L(\mathbf{q})$  and  $\varepsilon_T(\mathbf{q})$ .  $c_L(q) = \langle \varepsilon_L(\mathbf{q}) \varepsilon_L(-\mathbf{q}) \rangle_{\hat{\mathbf{q}}}$  and  $c_T(q) = \langle \varepsilon_T(\mathbf{q}) \varepsilon_T(-\mathbf{q}) \rangle_{\hat{\mathbf{q}}}$  are computed by averaging over all  $c$  and  $t$  and all wavevectors  $\mathbf{q}$  with magnitude  $|\mathbf{q}|$

within a chosen bin around  $q$ . The correlation functions  $c_{\alpha\beta\gamma\delta}(\mathbf{r})$  in real space (either for unrotated or  $\alpha$ -rotated coordinate systems) are finally obtained by inverse FFT.

#### Appendix D: Macroscopic elastic properties

The amorphous glasses formed by pLJ particle systems at a pressure  $P = 2$  and a temperature  $T = 0.2 \ll T_g \approx 0.26$  can be viewed for sampling (production) times  $\Delta\tau \leq 10^7$  MCS for all practical purposes as elastic bodies [17, 21, 35, 37, 49, 50]. Moreover, these systems can be shown to be isotropic above distances corresponding to a couple of particle diameters [17, 37]. We briefly summarize here their macroscopic linear elastic properties. It is well known that the free energy increment  $\delta F$  due to an applied external (small) strain  $\varepsilon_{\alpha\beta}$  is given by [7, 8]

$$\delta F/V = \frac{1}{2} \varepsilon_{\alpha\beta} E_{\alpha\beta\gamma\delta} \varepsilon_{\gamma\delta} \quad (\text{D1})$$

with  $E_{\alpha\beta\gamma\delta}$  being the forth-order elastic modulus tensor. The standard minor and major symmetries

$$E_{\alpha\beta\gamma\delta} = E_{\beta\alpha\gamma\delta} = E_{\alpha\beta\delta\gamma} = E_{\gamma\delta\alpha\beta} = \dots \quad (\text{D2})$$

with respect to the suffices are assumed. As already noted in Appendix A4, for isotropic systems  $E_{\alpha\beta\gamma\delta}$  is completely determined by *two* invariants, say the two isothermic Lamé moduli  $\lambda$  and  $\mu$ . In agreement with Eq. (A14)  $E_{\alpha\beta\gamma\delta}$  may thus be written [7, 8]

$$E_{\alpha\beta\gamma\delta} = \lambda \delta_{\alpha\beta} \delta_{\gamma\delta} + \mu (\delta_{\alpha\gamma} \delta_{\beta\delta} + \delta_{\alpha\delta} \delta_{\beta\gamma}). \quad (\text{D3})$$

Note that  $E_{1111} = E_{2222} = \lambda + 2\mu$ ,  $E_{1122} = \lambda$  and  $E_{1212} = \mu$ . As described in detail elsewhere [21, 35, 49–52] we have determined  $\lambda$  and  $\mu$  either by means of strain fluctuations, e.g., by letting the box volume  $V$  fluctuate at imposed pressure  $P$  [49], or using the stress-fluctuation formalism at fixed volume and shape of the simulation box [51, 52]. This shows for all methods that  $\lambda \approx 38$  and  $\mu \approx 14$ . We have verified that

- similar values are obtained for  $n \geq 5000$ ,
- similar values are obtained using different components, say  $E_{1111}$  and  $E_{2222}$  for  $\lambda + 2\mu$ , and
- the fluctuations of  $E_{\alpha\beta\gamma\delta}|_c$  for independent configurations  $c$  become negligible for  $n \geq 5000$ .

#### Appendix E: Microscopic elastic tensor fields

We turn now to the relevant microscopic tensor fields as functions of either the spatial position  $\mathbf{r}$  (real space) or the wavevector  $\mathbf{q}$  (reciprocal space).

## 1. Displacement fields

As in previous experimental and numerical studies [9, 10, 21] the displacement field  $\mathbf{u}(\mathbf{r})$  in real space is constructed from the instantaneous spatial positions  $\mathbf{r}_a$  of the particles  $a$  with respect to their reference positions  $\tilde{\mathbf{r}}_a$ . Both  $\mathbf{r}_a$  and  $\tilde{\mathbf{r}}_a$  are computed at constant center-of-mass of all particles. As reference position  $\tilde{\mathbf{r}}_a$  we have used either the average particle position determined using a long trajectory or the particle position after a rapid quench to  $T = 0$ . Having not observed any significant quantitative difference between both methods we only report here data computed using the first one. We thus obtain the displacement vector  $\mathbf{u}_a = \mathbf{r}_a - \tilde{\mathbf{r}}_a$  for each  $a$ . By construction the average displacement vector  $\langle \mathbf{u}_a \rangle$  must vanish. We find

$$u_{\text{rms}} \equiv \langle \mathbf{u}_a^2 \rangle^{1/2} \approx 0.13 \quad (\text{E1})$$

for the root-mean-squared average  $u_{\text{rms}}$  (sampled over all particles, frames and configurations). The instantaneous displacement field may then be defined by [9, 10, 21]

$$\mathbf{u}(\mathbf{r}) = \frac{1}{n/V} \sum_a \mathbf{u}_a \delta(\mathbf{r} - \tilde{\mathbf{r}}_a) \quad (\text{E2})$$

assuming for the moment an infinitesimal fine grid, i.e.  $a_{\text{grid}} \rightarrow 0$ . (Different prefactors have been used in Refs. [9, 10, 21].) We remind that the  $\delta(\mathbf{r})$ -function has the dimension “1/volume”. By definition  $\mathbf{u}(\mathbf{r})$  has thus the same dimension “length” as the displacement vector  $\mathbf{u}_a$ . Following the common definition of the particle flux density [33], the reference position  $\tilde{\mathbf{r}}_a$  in the  $\delta$ -function may be replaced by the time-dependent position  $\mathbf{r}_a$ , i.e. the displacement field may alternatively be defined by

$$\mathbf{u}(\mathbf{r}) = \frac{1}{n/V} \sum_a \mathbf{u}_a \delta(\mathbf{r} - \mathbf{r}_a). \quad (\text{E3})$$

Both operational definitions are compared for the transverse ICF  $\beta V c_T(q)$  in Fig. 6 where data obtained using Eq. (E2) are indicated by open symbols. In reciprocal space we obtain

$$\mathbf{u}(\mathbf{q}) = \frac{1}{n} \sum_a \mathbf{u}_a \exp(-i\mathbf{q} \cdot \tilde{\mathbf{r}}_a). \quad (\text{E4})$$

for Eq. (E2) and similarly for Eq. (E3) with  $\mathbf{r}_a$  replacing  $\tilde{\mathbf{r}}_a$ . Since  $\mathbf{r}_a = \tilde{\mathbf{r}}_a + \mathbf{u}_a$  we have to leading order

$$\exp(-i\mathbf{q} \cdot \mathbf{r}_a) \approx \exp(-i\mathbf{q} \cdot \tilde{\mathbf{r}}_a) (1 - i\mathbf{q} \cdot \mathbf{u}_a \dots) \quad (\text{E5})$$

for  $q|\mathbf{u}(\mathbf{q})| \ll 1$ . Both operational definitions Eq. (E2) and Eq. (E3) thus should become equivalent for  $qu_{\text{rms}} \ll 1$ . Due to the small typical (root-mean-squared) displacement  $u_{\text{rms}}$ , Eq. (E1), this holds for all sampled  $q$  as may be seen from the data presented in Fig. 6. Due to the center-of-mass convention the volume integral over  $\mathbf{u}(\mathbf{r})$  must vanish and, equivalently, we have  $\mathbf{u}(\mathbf{q} = 0) = 0$  in

reciprocal space for each instantaneous field. We also remind that the two coordinates of the displacement field in NRC are the longitudinal component  $u_L(\mathbf{q}) \equiv u_1^o(\mathbf{q})$  and the transverse component  $u_T(\mathbf{q}) \equiv u_2^o(\mathbf{q})$ .

In numerical practice, the continuous field vector  $\mathbf{r}$  of Eq. (E2) and Eq. (E3) corresponds to the discrete point on the grid, Eq. (B10), closest (using the minimal image convention) to, respectively, the reference position  $\tilde{\mathbf{r}}_a$  or the particle position  $\mathbf{r}_a$ . Strictly speaking, we thus obtain by means of Eq. (B8) the Fourier transform with respect to their respective closest grid points [53]. The differences between these definitions become negligible for  $qa_{\text{grid}} \ll 1$ . That this holds can be clearly seen from Fig. 6 where we have varied  $a_{\text{grid}}$  over more than one order of magnitude.

## 2. Linear strain field

Using the displacement field  $\mathbf{u}(\mathbf{r})$  the linear (“small”) strain tensor field is defined by [7, 8]

$$\varepsilon_{\alpha\beta}(\mathbf{r}) \equiv \frac{1}{2} \left( \frac{\partial u_\alpha(\mathbf{r})}{\partial r_\beta} + \frac{\partial u_\beta(\mathbf{r})}{\partial r_\alpha} \right). \quad (\text{E6})$$

Due to Eq. (B3) this becomes

$$\varepsilon_{\alpha\beta}(\mathbf{q}) = \frac{i}{2} (q_\beta u_\alpha(\mathbf{q}) + q_\alpha u_\beta(\mathbf{q})). \quad (\text{E7})$$

in reciprocal space. (Obviously,  $\varepsilon_{\alpha\beta} = \varepsilon_{\beta\alpha}$  for any  $\mathbf{r}$  in real space and any  $\mathbf{q}$  in reciprocal space.) Note that both  $\varepsilon_{\alpha\beta}(\mathbf{r})$  and its Fourier transform  $\varepsilon_{\alpha\beta}(\mathbf{q})$ , cf. Eq. (B1), are dimensionless fields. Due to our definitions and conventions the macroscopic strain  $\varepsilon_{\alpha\beta}(\mathbf{q} = 0)$  is assumed to vanish. Using Eq. (E7) we numerically determine the three relevant components of the (symmetric) strain tensor field  $\varepsilon_{\alpha\beta}(\mathbf{q})$  from the two components of the displacement field  $u_\alpha(\mathbf{q})$  stored on the reciprocal space grid (cf. Fig. 5) and the wavevector  $q_\alpha$  according to Eq. (B10). It follows from Eq. (E7) that

$$\varepsilon_{22}^o(\mathbf{q}) = 0, \quad (\text{E8})$$

$$\varepsilon_{11}^o(\mathbf{q}) \equiv \varepsilon_L(\mathbf{q}) = iqu_L(\mathbf{q}), \quad (\text{E9})$$

$$\varepsilon_{12}^o(\mathbf{q}) \equiv \varepsilon_{21}^o(\mathbf{q}) \equiv \varepsilon_T(\mathbf{q}) = iqu_T(\mathbf{q})/2 \quad (\text{E10})$$

in NRC for all  $\mathbf{q}$ . Hence, the longitudinal strains and displacement fields are equivalent and the same applies to the two transverse fields. Numerically, we first obtain  $u_L(\mathbf{q})$  and  $u_T(\mathbf{q})$  and from this  $\varepsilon_L(\mathbf{q})$  and  $\varepsilon_T(\mathbf{q})$ .

## 3. Free energy density field $f(\mathbf{q})$

The total (inner) free energy per volume of the system may be written as the sum

$$\delta F/V = \sum_{\mathbf{q}} f(\mathbf{q}) \quad (\text{E11})$$

over free energy contributions  $f(\mathbf{q})$  per volume for different wavevectors  $\mathbf{q}$  [6]. As reminded below, in two dimensions  $f(\mathbf{q})$  becomes the sum of two independent free energy contributions  $f_L(\mathbf{q})$  and  $f_T(\mathbf{q})$  associated with the two independent longitudinal and transverse displacement fields  $u_L(\mathbf{q})$  and  $u_T(\mathbf{q})$  in NRC. Let us begin by stating the free energy density in reciprocal space

$$f(\mathbf{q}) = \frac{1}{2} \varepsilon_{\alpha\beta}(\mathbf{q}) E_{\alpha\beta\gamma\delta}(\mathbf{q}) \varepsilon_{\gamma\delta}^*(\mathbf{q}) \quad (\text{E12})$$

using the standard (yet not rotated) coordinate system and denoting the conjugate complex of a number by “ $\star$ ”.  $E_{\alpha\beta\gamma\delta}(\mathbf{q})$  stands here for a generalization (defined below) of the macroscopic elastic modulus tensor  $E_{\alpha\beta\gamma\delta}$  (without argument) stated above. The standard minor and major symmetries, Eq. (D2), with respect to the suffices are now assumed to hold for all  $\mathbf{q}$ . Using the major suffix symmetry it is seen that

$$f(\mathbf{q}) = f^*(\mathbf{q}) = f(-\mathbf{q}), \quad (\text{E13})$$

i.e.  $f(\mathbf{q})$  is a real number and the free energy densities for  $\mathbf{q}$  and  $-\mathbf{q}$  are identical. This is expected since the opposite wavevectors characterize exactly the same fluctuation as discussed, e.g., in Ref. [40]. (We come back to this issue in Appendix E4.) It can be argued [16] that  $E_{\alpha\beta\gamma\delta}(\mathbf{q}) \rightarrow E_{\alpha\beta\gamma\delta}$  in a continuous manner in the small- $\mathbf{q}$  limit. Moreover, for isotropic systems  $E_{\alpha\beta\gamma\delta}(\mathbf{q})$  must be an isotropic forth-order tensor field, cf. Eq. (A19). It can be shown that for isotropic achiral systems [16]

$$\begin{aligned} E_{\alpha\beta\gamma\delta}(\mathbf{q}) = & M(q) \delta_{\alpha\beta} \delta_{\gamma\delta} \\ & + G(q) [\delta_{\alpha\gamma} \delta_{\beta\delta} + \delta_{\alpha\delta} \delta_{\beta\gamma}] \\ & + [L(q) - 2G(q) - M(q)] \\ & \times [\hat{q}_\alpha \hat{q}_\beta \delta_{\gamma\delta} + \hat{q}_\gamma \hat{q}_\delta \delta_{\alpha\beta} - \delta_{\alpha\beta} \delta_{\gamma\delta}] \end{aligned} \quad (\text{E14})$$

setting thus for the invariants of Eq. (A19)

$$\begin{aligned} i_1(q) &= M(q) - i_3(q) \\ i_2(q) &= G(q), \\ i_3(q) &= L(q) - 2G(q) - M(q) \text{ and} \\ i_4(q) &= i_5(q) = 0. \end{aligned} \quad (\text{E15})$$

Interestingly, for isotropic systems  $E_{\alpha\beta\gamma\delta}(\mathbf{q})$  depends not only on two but on *three* independent invariants. These “material functions” are the “longitudinal modulus”  $L(q)$ , the “mixed modulus”  $M(q)$  and the (generalized) “shear modulus”  $G(q)$  [16]. Note that

$$L(q) \rightarrow \lambda + 2\mu, M(q) \rightarrow \lambda, G(q) \rightarrow \mu \text{ for } q \rightarrow 0, \quad (\text{E16})$$

i.e.  $i_3(q) \rightarrow 0$  and  $E_{\alpha\beta\gamma\delta}(\mathbf{q})$  reduces to Eq. (D3) for large wavelengths. Importantly,  $f(\mathbf{q})$  is a scalar field, i.e. its value does not depend on the coordinate system. We may compute it most readily in NRC where

$$f(\mathbf{q}) = \frac{1}{2} \varepsilon_{\alpha\beta}^\circ(\mathbf{q}) E_{\alpha\beta\gamma\delta}^\circ(\mathbf{q}) \varepsilon_{\gamma\delta}^\circ(-\mathbf{q}). \quad (\text{E17})$$

We note that

$$\begin{aligned} E_{1111}^\circ(\mathbf{q}) &= i_1(q) + 2i_2(q) + 2i_3(q) + i_4(q) = L(q), \\ E_{2222}^\circ(\mathbf{q}) &= i_1(q) + 2i_2(q) = 4G(q) + 2M(q) - L(q), \\ E_{1122}^\circ(\mathbf{q}) &= i_1(q) + i_3(q) = M(q), \\ E_{1212}^\circ(\mathbf{q}) &= i_2(q) = G(q) \text{ and} \\ E_{1112}^\circ(\mathbf{q}) &= E_{1222}^\circ(\mathbf{q}) = E_{1211}^\circ(\mathbf{q}) = \dots = 0 \end{aligned}$$

in agreement with Eq. (A20) and Eq. (A21). Using also that  $\varepsilon_{12}^\circ(\mathbf{q}) = \varepsilon_{21}^\circ(\mathbf{q})$  and  $\varepsilon_{22}^\circ(\mathbf{q}) = 0$  it is seen that

$$f(\mathbf{q}) = f_L(\mathbf{q}) + f_T(\mathbf{q}) \text{ with} \quad (\text{E18})$$

$$f_L(\mathbf{q}) = \frac{L(q)}{2} \varepsilon_L(\mathbf{q}) \varepsilon_L^*(\mathbf{q}) \text{ and} \quad (\text{E19})$$

$$f_T(\mathbf{q}) = \frac{4G(q)}{2} \varepsilon_T(\mathbf{q}) \varepsilon_T^*(\mathbf{q}) \quad (\text{E20})$$

for the two independent longitudinal and transverse free energy contributions [54]. As can be seen from the two previous relations, the free energy contributions in reciprocal space are not only real but according to the Wiener-Khinchin theorem, Eq. (B7), also *positive-definite*. Being scalars this holds for any orthogonal transformation.

#### 4. Strain distributions in NRC

We turn now to the probability distributions of the strains controlled by these two free energy contributions. As already noted, the fluctuation modes for wavevectors  $\mathbf{q}$  and  $-\mathbf{q}$  are perfectly correlated [40]. The Maxwell-Boltzmann weights for the longitudinal and transverse modes for  $\mathbf{q}$  are thus given by

$$p(\varepsilon_L(\mathbf{q})) \propto e^{-\beta V [f_L(\mathbf{q}) + f_L(-\mathbf{q})]} \text{ and} \quad (\text{E21})$$

$$p(\varepsilon_T(\mathbf{q})) \propto e^{-\beta V [f_T(\mathbf{q}) + f_T(-\mathbf{q})]}. \quad (\text{E22})$$

Using Eq. (E13), Eq. (E19) and Eq. (E20) this yields

$$p(\varepsilon_L(\mathbf{q})) = \frac{\beta V L(q)}{\pi} e^{-\beta V L(q) \varepsilon_L(\mathbf{q}) \varepsilon_L^*(\mathbf{q})} \text{ and} \quad (\text{E23})$$

$$p(\varepsilon_T(\mathbf{q})) = \frac{\beta V 4G(q)}{\pi} e^{-\beta V 4G(q) \varepsilon_T(\mathbf{q}) \varepsilon_T^*(\mathbf{q})}, \quad (\text{E24})$$

i.e. the complex random variables  $\varepsilon_L(\mathbf{q})$  and  $\varepsilon_T(\mathbf{q})$  have complex circularly-symmetric Gaussian probability distributions [55]. Using, moreover, that

$$\langle zz^* \rangle = \frac{1}{a} \text{ if } p(z) = \frac{a}{\pi} \exp(-az z^*) \quad (\text{E25})$$

for a complex random variable  $z$  [40], the above two distributions imply the general equipartition relations

$$\beta V c_L(q) = \frac{1}{L(q)} \text{ and } \beta V c_T(q) = \frac{1}{4G(q)} \quad (\text{E26})$$

connecting the two independent strain fluctuations in NRC with the two material functions  $L(q)$  and  $G(q)$ .

These equipartition relations may be used to obtain  $L(q)$  and  $G(q)$  as will be discussed elsewhere [56]. According to Eq. (E16)  $L(q) \rightarrow \lambda + 2\mu$  and  $G(q) \rightarrow \mu$  for small  $q$ . This limit of the equipartition theorem, Eq. (4), has been used in the main part of this work.

### 5. Strain distributions in original frame

Let us return to the original coordinate frame. Using Eq. (A2)  $\varepsilon_{\alpha\beta}(\mathbf{q})$  may be expressed as

$$\begin{aligned}\varepsilon_{11}(\mathbf{q}) &= c^2 \varepsilon_{11}^\circ(\mathbf{q}) + s^2 \varepsilon_{22}^\circ(\mathbf{q}) - 2sc \varepsilon_{12}^\circ(\mathbf{q}) \\ &= c^2 \varepsilon_L(\mathbf{q}) - 2sc \varepsilon_T(\mathbf{q})\end{aligned}\quad (\text{E27})$$

$$\begin{aligned}\varepsilon_{22}(\mathbf{q}) &= s^2 \varepsilon_{11}^\circ(\mathbf{q}) + c^2 \varepsilon_{22}^\circ(\mathbf{q}) + 2sc \varepsilon_{12}^\circ(\mathbf{q}) \\ &= s^2 \varepsilon_L(\mathbf{q}) + 2sc \varepsilon_T(\mathbf{q})\end{aligned}\quad (\text{E28})$$

$$\begin{aligned}\varepsilon_{12}(\mathbf{q}) &= sc \varepsilon_{11}^\circ(\mathbf{q}) - sc \varepsilon_{22}^\circ(\mathbf{q}) + (c^2 - s^2) \varepsilon_{12}^\circ(\mathbf{q}) \\ &= cs \varepsilon_L(\mathbf{q}) + (c^2 - s^2) \varepsilon_T(\mathbf{q})\end{aligned}\quad (\text{E29})$$

in terms of the longitudinal and transverse strains  $\varepsilon_L(\mathbf{q})$  and  $\varepsilon_T(\mathbf{q})$  in NRC with  $c = \cos(\theta) = \hat{q}_1$  and  $s = \sin(\theta) = \hat{q}_2$  being coefficients depending only on the wavevector angle  $\theta$ . Since  $\varepsilon_L(\mathbf{q})$  and  $\varepsilon_T(\mathbf{q})$  are complex circularly-symmetric Gaussian distributed random numbers, the same thus applies (with different coefficients) for the strains  $\varepsilon_{\alpha\beta}(\mathbf{q})$ . While the distributions of  $\varepsilon_L(\mathbf{q})$  and  $\varepsilon_T(\mathbf{q})$  do not depend on  $\theta$  (being completely characterized by the ICFs) the wavevector direction obviously matters for the distributions of  $\varepsilon_{\alpha\beta}(\mathbf{q})$ . The Gaussianity of  $\varepsilon_{\alpha\beta}(\mathbf{q})$  implies due to Eq. (B2) that also their (real valued) inverse Fourier transforms  $\varepsilon_{\alpha\beta}(\mathbf{r})$  must be Gaussian (centered around the origin of the real axis). Since all spatial positions  $\mathbf{r}$  are equivalent (translational invariance) the latter distributions do not depend on  $\mathbf{r}$  (neither on its magnitude or direction).

#### Appendix F: From $c_L(q)$ and $c_T(q)$ to $c_{\alpha\beta\gamma\delta}(\mathbf{r})$

As shown in Appendix A 5, a forth-order tensor field describing an isotropic achiral system in two dimensions is given by the general relation Eq. (A19) in terms of four invariants  $i_n(q)$ . In turn these invariants are expressed, Eq. (A22), in terms of the alternative set of invariants  $c_L(q)$ ,  $c_T(q)$ ,  $c_2(q)$  and  $c_T(q)$ . Due to Eq. (E8) we have  $c_2(q) = c_\perp(q) = 0$  for strain correlations. The correlation function  $c_{\alpha\beta\gamma\delta}(\mathbf{q})$  in reciprocal space are thus given by the invariants

$$-\frac{i_1(q)}{2} = \frac{i_3(q)}{2} = i_2(q) = c_T(q) \text{ and} \quad (\text{F1})$$

$$i_4(q) = c_L(q) - 4c_T(q). \quad (\text{F2})$$

More specifically, this implies

$$\begin{aligned}c_{1111}(\mathbf{q}) &= c^4 c_L(q) + 4s^2 c^2 c_T(q) \\ c_{2222}(\mathbf{q}) &= s^4 c_L(q) + 4s^2 c^2 c_T(q) \\ c_{1122}(\mathbf{q}) &= c^2 s^2 c_L(q) - 4s^2 c^2 c_T(q) \\ c_{1212}(\mathbf{q}) &= c^2 s^2 c_L(q) + (c^2 - s^2)^2 c_T(q) \\ c_{1112}(\mathbf{q}) &= c^3 c_L(q) - 2sc(c^2 - s^2) c_T(q) \\ c_{1222}(\mathbf{q}) &= cs^3 c_L(q) + 2sc(c^2 - s^2) c_T(q)\end{aligned}\quad (\text{F3})$$

using again the  $\theta$ -dependent coefficients  $c$  and  $s$  introduced above. The latter six relations may also be directly obtained using that the components  $\varepsilon_{\alpha\beta}(\mathbf{q})$  in the original coordinate frame can be expressed in terms of the longitudinal and transverse strains  $\varepsilon_L(\mathbf{q})$  and  $\varepsilon_T(\mathbf{q})$ , Eqs. (E27-E29), and that  $\varepsilon_L(\mathbf{q})$  and  $\varepsilon_T(\mathbf{q})$  fluctuate independently. For the correlation functions  $c'_{\alpha\beta\gamma\delta}(\mathbf{q})$  in rotated coordinate systems one simply replaces  $\theta$  by  $x = \theta - \alpha$ . Note also that  $c'_{1112}(\mathbf{q})$  and  $c'_{1222}(\mathbf{q})$  do in general not vanish for all  $x$  in standard (unrotated or rotated) coordinates. The values for NRC are obtained by setting  $x = 0$ , i.e.  $s = 0$  and  $c = 1$ .

We expand the angle-dependent coefficients of  $c_L(q)$  and  $c_T(q)$  in terms of the Fourier modes  $\cos(p\theta)$  and  $\sin(p\theta)$  with  $p$  being integers using that

$$\begin{aligned}cs &= \sin(2\theta)/2, \\ c^4 &= \frac{1}{8} (\cos(4\theta) + 4\cos(2\theta) + 3), \\ s^4 &= \frac{1}{8} (\cos(4\theta) - 4\cos(2\theta) + 3), \\ c^2 s^2 &= \frac{1}{8} (1 - \cos(4\theta)) \text{ and} \\ (c^2 - s^2)^2 &= 1 - 4c^2 s^2 = \frac{1}{2} (1 + \cos(4\theta)).\end{aligned}$$

This implies for example

$$\begin{aligned}c_{1212} &= \frac{1}{8} [(4c_T - c_L) \cos(4\theta) + (4c_T + c_L)] \\ c_{1122} &= \frac{1}{8} [(4c_T - c_L) \cos(4\theta) - (4c_T + c_L)] \\ \frac{c_{1111} + c_{2222}}{2} &= \frac{1}{8} [-(4c_T - c_L) \cos(4\theta) + 3c_L + 4c_T] \\ \frac{c_{1111} - c_{2222}}{2} &= \frac{1}{4} (2c_L) \cos(2\theta) \\ \frac{c_{1112} + c_{1222}}{2} &= \frac{1}{4} c_L(q) \sin(2\theta) \\ \frac{c_{1112} - c_{1222}}{2} &= -\frac{1}{8} [4c_T - c_L] \sin(4\theta)\end{aligned}$$

where we have omitted the arguments  $\mathbf{q}$  on the l.h.s. and  $q$  on the r.h.s. The prefactor of  $\cos(4\theta)$  and  $\sin(4\theta)$  is always proportional to  $i_4(q)$ . We remind that the ICFs  $c_L(q)$  and  $c_T(q)$  are related to the elastic material functions  $L(q)$  and  $G(q)$ , Eq. (E26). If  $L(q)$  and  $G(q)$  are known we thus have  $c_{\alpha\beta\gamma\delta}(\mathbf{q})$  and by inverse Fourier transform (at least numerically)  $c_{\alpha\beta\gamma\delta}(\mathbf{r})$  in real space.

Importantly,  $L(q) \rightarrow \lambda + 2\mu$  and  $G(q) \rightarrow \mu$  become constant in the low- $q$  limit. We introduce for convenience the constants  $J_1$  and  $J_2$  defined by

$$\beta V[4c_T(q) - c_L(q)] \rightarrow J_1 \equiv \frac{1}{\mu} - \frac{1}{\lambda + 2\mu}, \quad (\text{F4})$$

$$\beta V[2c_L(q)] \rightarrow J_2 \equiv \frac{2}{\lambda + 2\mu} \quad (\text{F5})$$

in the low- $q$  limit. We thus get in reciprocal space

$$\begin{aligned} \beta V c_{1212}(\mathbf{q}) &\rightarrow \frac{J_1}{8} \cos(4\theta) + \dots \\ \beta V c_{1122}(\mathbf{q}) &\rightarrow \frac{J_1}{8} \cos(4\theta) + \dots \\ \beta V \frac{c_{1111}(\mathbf{q}) + c_{2222}(\mathbf{q})}{2} &\rightarrow -\frac{J_1}{8} \cos(4\theta) + \dots \\ \beta V \frac{c_{1111}(\mathbf{q}) - c_{2222}(\mathbf{q})}{2} &\rightarrow \frac{J_2}{4} \cos(2\theta) \\ \beta V \frac{c_{1112}(\mathbf{q}) + c_{1222}(\mathbf{q})}{2} &\rightarrow \frac{J_2}{8} \sin(2\theta) \\ \beta V \frac{c_{1112}(\mathbf{q}) - c_{1222}(\mathbf{q})}{2} &\rightarrow \frac{J_1}{8} \sin(4\theta) \end{aligned}$$

where the dots mark constant terms. These terms are irrelevant for the inverse Fourier transform, only leading to contributions at the origin  $\mathbf{r} = \mathbf{0}$ . We may thus take advantage of the analytical result for the inverse Fourier transform of  $\cos(p\theta)$  and  $\sin(p\theta)$ , Eq. (B16), for  $p = 2$  and  $p = 4$ . Finally, we thus obtain the large- $r$  limits

$$\beta c_{1212}(\mathbf{r}) \rightarrow \frac{J_1}{4\pi r^2} \cos(4\theta) \quad (\text{F6})$$

$$\beta c_{1122}(\mathbf{r}) \rightarrow \frac{J_1}{4\pi r^2} \cos(4\theta) \quad (\text{F7})$$

$$\beta \frac{c_{1111}(\mathbf{r}) + c_{2222}(\mathbf{r})}{2} \rightarrow -\frac{J_1}{4\pi r^2} \cos(4\theta) \quad (\text{F8})$$

$$\beta \frac{c_{1111}(\mathbf{r}) - c_{2222}(\mathbf{r})}{2} \rightarrow -\frac{J_2}{4\pi r^2} \cos(2\theta) \quad (\text{F9})$$

$$\beta \frac{c_{1112}(\mathbf{r}) + c_{1222}(\mathbf{r})}{2} \rightarrow -\frac{J_2/2}{4\pi r^2} \sin(2\theta) \quad (\text{F10})$$

$$\beta \frac{c_{1112}(\mathbf{r}) - c_{1222}(\mathbf{r})}{2} \rightarrow -\frac{J_1}{4\pi r^2} \sin(2\theta) \quad (\text{F11})$$

with  $\theta$  denoting the polar angle of the field vector  $\mathbf{r}$ . The correlation functions  $c'_{\alpha\beta\gamma\delta}(\mathbf{r})$  in rotated coordinate systems generalize the above equations by substituting  $\theta$  with the angle difference  $x = \theta - \alpha$ . These results can be rewritten compactly using the general form expected from Eq. (A23) for a manifest two-dimensional, isotropic and achiral forth-order tensor field in real space yielding

$$\begin{aligned} \beta c'_{\alpha\beta\gamma\delta}(\mathbf{r}) &= \tilde{i}_1(r) \delta_{\alpha\beta} \delta_{\gamma\delta} \\ &+ \tilde{i}_2(r) [\delta_{\alpha\gamma} \delta_{\beta\delta} + \delta_{\alpha\delta} \delta_{\beta\gamma}] \\ &+ \tilde{i}_3(r) [\hat{r}'_{\alpha} \hat{r}'_{\beta} \delta_{\gamma\delta} + \hat{r}'_{\gamma} \hat{r}'_{\delta} \delta_{\alpha\beta}] \\ &+ \tilde{i}_4(r) \hat{r}'_{\alpha} \hat{r}'_{\beta} \hat{r}'_{\gamma} \hat{r}'_{\delta} \end{aligned} \quad (\text{F12})$$

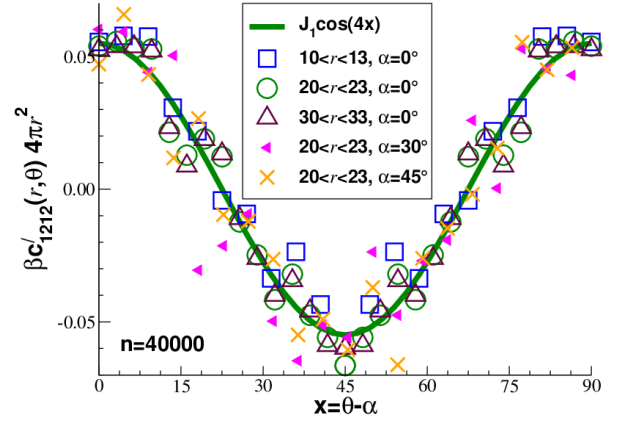


FIG. 7: Rescaled shear-strain autocorrelation function  $\beta c'_{1212}(r, \theta) 4\pi r^2$  in real space as a function of  $x = \theta - \alpha$  comparing data for different  $r$ -intervals and rotation angles  $\alpha$  with the prediction (bold solid line).

where the invariants  $\tilde{i}_n(r)$  in real space are given by

$$\begin{aligned} 4\pi r^2 \tilde{i}_1(r) &= J_2 - 3J_1, \\ 4\pi r^2 \tilde{i}_2(r) &= J_1, \\ 4\pi r^2 \tilde{i}_3(r) &= 4J_1 - J_2 \text{ and} \\ 4\pi r^2 \tilde{i}_4(r) &= -8J_1. \end{aligned} \quad (\text{F13})$$

Since  $i_1 = -(2J_1 + J_2)/4$ ,  $i_2 = (2J_1 + J_2)/8$ ,  $i_3 = (2J_1 + J_2)/4$  and  $i_4 = -J_1$ , this is consistent with the more general relation Eq. (A24).

The angle dependence for the shear-strain autocorrelation function in real space is investigated in Fig. 7 where we plot using linear coordinates  $\beta c'_{1212}(r, \theta) 4\pi r^2$  as a function of  $x$  for different  $r$  and  $\alpha$ . (To obtain sufficiently high statistics we need to average over the indicated finite  $r$ -bins. This is done by weighting each data entry for a bin with the proper factor  $4\pi r^2$ .) The data compare well with the prediction, Eq. (F6), confirming thus especially the scaling with angle difference  $x = \theta - \alpha$ . Naturally, the statistics deteriorates with increasing  $r$  due to the faster decay of the correlations as compared to the noise.

## Appendix G: Linear response to point stress

Correlation functions describe quite generally the linear response due to a small perturbation [6, 33, 34, 40]. More specifically, correlation functions of tensor fields describe the linear response of a tensorial field due to an imposed tensor field. Since the correlation functions are components of an isotropic tensor field, Eq. (A19), such a linear response in general depends on the direction of the field vector  $\mathbf{r}$  and on the orientation of the coordinate system. We discuss here this general point in more detail focusing, naturally, on correlation functions  $c_{\alpha\beta\gamma\delta}(\mathbf{r})$  of the (linear) strain tensor field  $\varepsilon_{\alpha\beta}(\mathbf{r})$ .

According to the ‘‘Fluctuation Dissipation Theorem’’ (FDT) [33, 34, 40] the mean strain increment  $\delta\varepsilon_{\alpha\beta}(\mathbf{r})$



induced by an (externally imposed) static stress field  $\delta\sigma_{\alpha\beta}(\mathbf{r})$  can be written as the volume integral

$$\delta\varepsilon_{\alpha\beta}(\mathbf{r}) = \beta \int d\mathbf{r}' c_{\alpha\beta\gamma\delta}(\mathbf{r} - \mathbf{r}') \delta\sigma_{\gamma\delta}(\mathbf{r}') \quad (\text{G1})$$

where (as always) summation over repeated indices is implied. Note that imposing an external field  $\delta\sigma_{\alpha\beta}(\mathbf{r})$  corresponds to adding the perturbation term

$$- \int d\mathbf{r} \delta\sigma_{\alpha\beta}(\mathbf{r}) \varepsilon_{\alpha\beta}(\mathbf{r}) \quad (\text{G2})$$

to the Hamiltonian of the system. This is equivalent to the application of an appropriate external perturbative force field to each particle. According to the product theorem of isotropic tensor fields, Eq. (A7),  $\delta\varepsilon_{\alpha\beta}(\mathbf{r})$  must be an isotropic tensor field, if both  $c_{\alpha\beta\gamma\delta}(\mathbf{r})$  and  $\delta\sigma_{\alpha\beta}(\mathbf{r})$  are isotropic tensor fields. In this case

$$\delta\varepsilon_{\alpha\beta}(\mathbf{r}) = \tilde{k}_1(r)\delta_{\alpha\beta} + \tilde{k}_2(r)\hat{r}_\alpha\hat{r}_\beta \text{ for } r > 0 \quad (\text{G3})$$

must hold slightly rewriting Eq. (A16). While  $c_{\alpha\beta\gamma\delta}(\mathbf{r})$  must be an isotropic tensor field for isotropic systems, this may *a priori* not hold for the external source field.

Let us assume for convenience a point-like perturbation at the origin given by

$$\delta\sigma_{\alpha\beta}(\mathbf{r}) = s_{\alpha\beta}\delta(\mathbf{r}) \quad (\text{G4})$$

with  $s_{\alpha\beta}$  being a symmetric  $2 \times 2$  matrix (of dimension “stress  $\times$  volume = energy”). Note that the symmetric tensor  $s_{\alpha\beta}$  can be diagonalized by an appropriate rotation of the coordinate system. The perturbation effect of  $s_{\alpha\beta}$  is therefore equivalent to that of two small force dipoles oriented along the eigenvectors with strengths equal to the corresponding eigenvalues. Such a perturbation, Eq. (G4), can be achieved by insertion of a small particle (of ellipsoidal or arbitrary shape) at the origin. The point-like perturbation Eq. (G4) implies

$\delta\varepsilon_{\alpha\beta}(\mathbf{r}) = \beta c_{\alpha\beta\gamma\delta}(\mathbf{r}) s_{\gamma\delta}$ . Using Eq. (F12) and introducing the scalars  $s_1 = s_{\gamma\gamma}/2$  and  $s_2 = \hat{r}_\alpha s_{\alpha\beta} \hat{r}_\beta / 2$  we thus have

$$\begin{aligned} \delta\varepsilon_{\alpha\beta}(\mathbf{r}) &= 2 [\tilde{i}_1(r)s_1 + \tilde{i}_3(r)s_2] \delta_{\alpha\beta} \\ &+ 2\tilde{i}_2(r) s_{\alpha\beta} \\ &+ 2 [\tilde{i}_3(r)s_1 + \tilde{i}_4(r)s_2] \hat{r}_\alpha \hat{r}_\beta. \end{aligned} \quad (\text{G5})$$

Clearly, the term  $s_{\alpha\beta}$  in the second line must be isotropic to obtain an isotropic tensor field, Eq. (G3). This imposes  $s_{\alpha\beta} = s\delta_{\alpha\beta}$  corresponding to a spherical particle insertion. Hence,  $s_1 = s$  and  $s_2 = s/2$ . The two invariants in Eq. (G3) thus become

$$\begin{aligned} \tilde{k}_1(r)/s &= 2\tilde{i}_1(r) + 2\tilde{i}_2(r) + \tilde{i}_3(r) = \frac{J_2}{4\pi r^2} \\ \tilde{k}_2(r)/s &= 2\tilde{i}_3(r) + \tilde{i}_4(r) = -\frac{2J_2}{4\pi r^2} \end{aligned} \quad (\text{G6})$$

where we have used Eq. (F13) in the second step. We note that only the inverse modulus  $J_2$  associated with the longitudinal modes, cf. Eq. (F5), matters and all reference to statistical physics, i.e. the inverse temperature  $\beta$ , drops out (as it should). While in general an applied or measured stress will not be isotropic, this holds for the *average*  $\langle s_{\alpha\beta} \rangle = s\delta_{\alpha\beta}$  over source stresses with arbitrary orientations. In this case Eq. (G6) should be useful. The strain increments are thus expected to reveal *quadrupolar pattern* ( $p = 2$ ), e.g.,

$$\delta\varepsilon_{12}(\mathbf{r}) = s\beta c_{12\gamma\gamma}(\mathbf{r}) = -\frac{sJ_2}{4\pi r^2} \sin(2\theta) \quad (\text{G7})$$

for the shear-strain increment. At variance to this, the shear-strain autocorrelation function  $c_{1212}(\mathbf{r})$ , cf. Fig. 1 and Eq. (10), is *octupolar* ( $p = 4$ ).

The generalization of the above relations for isotropic and achiral tensor fields in higher dimensions  $d$  will be discussed elsewhere.

- 
- [1] A. J. McConnell, *Applications of Tensor Analysis* (Hassell Street Press, 2021).
  - [2] J. A. Schouten, *Tensor Analysis for Physicists* (Dover Publications, Oxford, 2015).
  - [3] W. Schultz-Piszachich, *Mathematik 11: Tensoralgebra und -analysis* (Verlag Harri Deutsch, Thun und Frankfurt/Main, 1977).
  - [4] R. Lambourne, *Relativity, Gravitation, and Cosmology* (Cambridge University Press, Cambridge, 2010).
  - [5] T. Frankel, *The Geometry of Physics. An Introduction* (Cambridge University Press, Cambridge, 2012), 3rd ed.
  - [6] P. M. Chaikin and T. C. Lubensky, *Principles of condensed matter physics* (Cambridge University Press, 1995).
  - [7] L. D. Landau and E. M. Lifshitz, *Theory of Elasticity* (Pergamon Press, New York, 1959).
  - [8] E. B. Tadmor, R. E. Miller, and R. S. Elliot, *Continuum Mechanics and Thermodynamics* (Cambridge University Press, Cambridge, 2012).
  - [9] C. Klix, F. Ebert, F. Weysser, M. Fuchs, G. Maret, and P. Keim, Phys. Rev. Lett. **109**, 178301 (2012).
  - [10] C. L. Klix, G. Maret, and P. Keim, Phys. Rev. X **5**, 041033 (2015).
  - [11] M. Maier, A. Zippelius, and M. Fuchs, Phys. Rev. Lett. **119**, 265701 (2017).
  - [12] M. Maier, A. Zippelius, and M. Fuchs, J. Chem. Phys. **149**, 084502 (2018).
  - [13] F. Vogel, A. Zippelius, and M. Fuchs, Europhys. Lett. **125**, 68003 (2019).
  - [14] A. Lemaître, J. Chem. Phys. **143**, 164515 (2015).
  - [15] A. Lemaître, J. Chem. Phys. **149**, 104107 (2018).
  - [16] L. Klochko, J. Baschnagel, J. P. Wittmer, and A. N. Semenov, Soft Matter **14**, 6835 (2018).
  - [17] L. Klochko, J. Baschnagel, J. Wittmer, H. Meyer,

- O. Benzerara, and A. N. Semenov, J. Chem. Phys. **156**, 164505 (2022).
- [18] D. Steffen, L. Schneider, M. Müller, and J. Rottler, J. Chem. Phys. **157**, 064501 (2022).
- [19] J. Wittmer, A. Semenov, and J. Baschnagel, Phys. Rev. Lett. (2023).
- [20] A. Kabla and G. Debrégeas, Phys. Rev. Lett. **90**, 258303 (2003).
- [21] J. P. Wittmer, H. Xu, O. Benzerara, and J. Baschnagel, Mol. Phys. **113**, 2881 (2015).
- [22] K. W. Desmond and E. R. Weeks, Phys. Rev. Lett. **115**, 098302 (2015).
- [23] G. Picard, A. Ajdari, F. Lequeux, and L. Bocquet, EPJE **15**, 371 (2004).
- [24] L. Bocquet, A. Colin, and A. Ajdari, Phys. Rev. Lett. **103**, 036001 (2009).
- [25] J. Chatteraj and A. Lemaître, Phys. Rev. Lett. **111**, 066001 (2013).
- [26] A. Nicolas, J. Rottler, and J.-L. Barrat, EPJE **37**, 1 (2014).
- [27] E. Flenner and G. Szamel, Phys. Rev. Lett. **114**, 025501 (2015).
- [28] B. Illing, S. Fritsch, D. Hajnal, C. Klix, P. Keim, and M. Fuchs, Phys. Rev. Lett. **117**, 208002 (2016).
- [29] M. Hassani, E. Zirdehi, K. Kok, P. Schall, M. Fuchs, and F. Varnik, Europhysics Letters **124**, 18003 (2018).
- [30] C. Liu, G. Biroli, D. R. Reichman, and G. Szamel, Phys. Rev. E **104**, 054606 (2021).
- [31] R. N. Chacko, F. P. Landes, G. Biroli, O. D. A. J. Liu, and D. R. Reichman, Phys. Rev. Lett. **127**, 048002 (2021).
- [32] M. P. Allen and D. J. Tildesley, *Computer Simulation of Liquids, 2nd Edition* (Oxford University Press, Oxford, 2017).
- [33] J. P. Hansen and I. R. McDonald, *Theory of simple liquids* (Academic Press, New York, 2006), 3rd edition.
- [34] D. Forster, *Hydrodynamic Fluctuations, Broken Symmetry, and Correlation Functions* (Perseus Books, New York, 1995).
- [35] J. P. Wittmer, H. Xu, P. Polńska, F. Weysser, and J. Baschnagel, J. Chem. Phys. **138**, 12A533 (2013).
- [36] L. Klochko, J. Baschnagel, J. P. Wittmer, and A. N. Semenov, J. Chem. Phys. **151**, 054504 (2019).
- [37] G. George, L. Klochko, A. Semenov, J. Baschnagel, and J. P. Wittmer, EPJE **44**, 13 (2021).
- [38] G. George, L. Klochko, A. N. Semenov, J. Baschnagel, and J. P. Wittmer, EPJE **44**, 54 (2021).
- [39] M. Rubinstein and R. H. Colby, *Polymer Physics* (Oxford University Press, Oxford, 2003).
- [40] M. Doi and S. F. Edwards, *The Theory of Polymer Dynamics* (Clarendon Press, Oxford, 1986).
- [41] J. K. G. Donth, *The Glass Transition: Relaxation dynamics in liquids and disordered materials* (Springer, Berlin-Heidelberg, 2001).
- [42] L. Klochko, J. Baschnagel, J. P. Wittmer, and A. N. Semenov, Soft Matter **17**, 7867 (2021).
- [43] A. Ninarello, L. Berthier, and D. Coslovich, Phys. Rev. X **7**, 021039 (2017).
- [44] See the Wikipedia entry on “Occam’s razor”.
- [45] J. Wittmer, A. Semenov, and J. Baschnagel, EPJE **45**, 65 (2022).
- [46] W. Press, S. Teukolsky, W. Vetterling, and B. Flannery, *Numerical Recipes in FORTRAN: the art of scientific computing* (Cambridge University Press, Cambridge, 1992).
- [47] M. Abramowitz and I. A. Stegun, *Handbook of Mathematical Functions* (Dover, New York, 1964).
- [48] The general (infinite) integral Eq. (11.4.16) of Ref. [47] is expressed in terms of two (in general complex) coefficients  $\mu$  and  $\nu$  which in our case take the (real) values  $\mu = 1$  and  $\nu = p$ . It is stated that Eq. (11.4.16) holds for  $\Re(\mu + \nu) > -1$ , being consistent with the condition  $p > -2$  noted in Eq. (B15), but also that  $\Re\mu < 1/2$ , being at first sight in conflict with  $\mu = 1$ . However, the integral divergence for  $t \rightarrow \infty$  for  $\mu > 1/2$  is fictitious as, e.g., discussed in the Wikipedia entry on “Oscillatory integrals” where it is noted that “*Oscillatory integrals make rigorous many arguments that, on a naive level, appear to use divergent integrals.*” Note especially that Eq. (B16) also holds for  $p = 0$  and finite  $r > 0$ . This simply follows from the well known fact that the Fourier transform of a constant is zero everywhere except at the origin. See Ref. [19] for an alternative more straight-forward but also more lengthy derivation of Eq. (B16) using the asymptotic behavior of the confluent hypergeometric Kummer function  $M(a, b, z)$ .
- [49] J. P. Wittmer, H. Xu, P. Polńska, C. Gillig, J. Helfferich, F. Weysser, and J. Baschnagel, Eur. Phys. J. E **36**, 131 (2013).
- [50] J. P. Wittmer, H. Xu, and J. Baschnagel, Phys. Rev. E **91**, 022107 (2015).
- [51] J. F. Lutsko, J. Appl. Phys. **64**, 1152 (1988).
- [52] J. F. Lutsko, J. Appl. Phys. **65**, 2991 (1989).
- [53] In principle one could directly without approximation compute the displacement field  $\mathbf{u}(\mathbf{q})$  using Eq. (E4) in reciprocal space. Unfortunately, this leads to an additional loop over all  $n$  particles for each wavevector  $\mathbf{q}$ .
- [54] The above argument generalizes for isotropic bodies in  $d \geq 2$  dimensions where Eq. (E18) becomes
- $$f(\mathbf{q}) = f_L(\mathbf{q}) + (d - 1)f_T(\mathbf{q})$$
- while Eq. (E19) and Eq. (E20) remain unchanged.
- [55] See the Wikipedia entry on “Complex normal distributions” for details and further references.
- [56] J. Wittmer, A. Semenov, and J. Baschnagel, under preparation (2023).